# On the Spectral Efficiency of LoRa Networks: Performance Analysis, Trends and Optimal Points of Operation

Lam-Thanh Tu, Abbas Bradai, Yannis Pousset

# On the Coverage Probability and Spectral Efficiency in LoRa Networks

Lam-Thanh Tu, Abbas Bradai and Yannis Pousset

**Abstract**

The coverage probability (Pcov) and the potential spectral efficiency (PSE) in LoRa networks are investigated. In particular, we propose an approximated but tractable mathematical framework by using tools from stochastic geometry and point processes. Based on the proposed framework, closed-form expressions for Pcov and PSE are provided. In addition, the impact of the average number of end-devices (EDs), the transmit power, the transmission bandwidth and the radius of the considered networks, are analyzed. Our findings reveal that Pcov and PSE have the same performance trends as a function of the transmit power, the radius of the networks and the transmission bandwidth. As for the average number of EDs, on the other hand, Pcov and PSE have a different behavior. Specifically, Pcov is a convex and monotonic decreasing property as a function of the number of EDs and the PSE is either a unimodal function or monotonic increasing function depending on the transmit power of the EDs. Moreover, a closed-form expression of the optimal number of EDs which maximizes the PSE is obtained. Finally, the proposed analytical frameworks and performance trends are validated with the aid of Monte Carlo simulations.

**Index Terms**

LoRa Networks, Stochastic Geometry, Coverage Probability, Spectral Efficiency.

## I. Introduction

It is expected that by the end of the year there will be over 50 billion end-devices (EDs) to be connected to the Internet that realizes the Internet-of-Things (IoTs) networks [2]. However, such this massive devices network also poses some challenges, e.g., how to support all devices with different quality-of-services (QoSs) levels simultaneously and how to cut down the power consumption as least as possible. At the first attempt, the cellular networks seems to be a wise choice with its well-standardised networks combined with super-dense deployment of the base stations (BSs). Nonetheless, such ultra-dense networks makes it too bulky and consume too much power as well. It, as a result, is essential to look for novel networks which is able to not only support a massive connected devices but also consume less power. Fortunately, low

L.-T. Tu, A. Bradai and Y. Pousset are with the Institute XLIM, University of Poitiers, France (email: lam.thanh.tu@univ-poitiers.fr; abbas.bradai@univ-poitiers.fr; yannis.pousset@univ-poitiers.fr). Parts of this paper have been accepted for presentation at IEEE International Conference on Communications 2020 [1].

power wide area network (LPWAN) has recently regarded as one of the promising networks thanks to its properties, e.g., low power consumption, low cost and wide coverage area. Compared with other available LPWAN technologies, i.e., Sigfox, NB-IoT, Weightless and so on, LoRa is considered as the most suitable one which attracts lots of attention from both academia and industry [3]. One of the main advantages of LoRa compared to other technologies is its patented modulation technology, i.e., the chirp spread spectrum (CSS) modulation [4], that has many benefits comparing with conventional modulations, e.g., PSK and QAM, respectively. Moreover, LoRa is also able to serve a large range of IoT applications with different QoS levels, i.e., e-Health, smart home, smart infrastructure monitoring and so forth, by actively fine-tuning its parameters, namely, the coding rate (CR), the spreading factor (SF), and the bandwidth (BW) and so forth. To further reduce the power consumption at end-devices, all kinds of synchronizations as well as sensing the availability of the medium are skipped in LoRa networks. It, as a consequence, allows end-devices to freely access the medium regardless of the channel occupancy. On the other hand, stochastic geometry (SG) is a mathematical tool which studies random point patterns. Hence, it is considered as a proper tool to evaluate the performance of wireless networks where the EDs and/or BSs are randomly distributed in a large area. Consequently, in the present paper, we address the performance of LoRa networks by utilizing tools from stochastic geometry. Before moving to the main contribution, some state-of-the-art of LoRa networks are discussed in the sequel.

One of the seminal works examining the performance of LoRa networks by using SG was in [5]. This work, nevertheless, did not take into account the correlation between noise and interference at the receiver. In [6], the performance of LoRa network with multiple receive antenna was studied. However, like in [5], the correlation between noise and interference were ignored. Moreover, it is apparent that multiple antennas seem to be impractical in LoRa networks as most of the EDs and/or gateway are low cost devices with simple hardware. Danielle *et al.* in [7] investigated the impact of imperfect orthogonality of LoRa networks. This work, however, focused on link-level that had a limited number of EDs. The symbol error rate and frame error rate were investigated, again, at link-level in [8]. The Pcov and potential spectral efficiency (PSE) were investigated in [9] by assuming that the EDs were distributed according to the Matern cluster process. Nevertheless, numerical computations were utilized to compute the system metrics rather than by using closed-form expressions; it, in addition, also constrained the paper's findings. To be more specific, all insights were drawn based on numerical computations in lieu of the mathematical framework which heavily relied on the simulation setups. The energy efficiency resource allocation of LoRa networks was addressed in [10] and a distributed network slicing strategy was proposed in [11] to address the question of scalability of large-scale LoRa networks.

In this paper, different to these above-mentioned works, we capitalize on the mathematical

tools of stochastic geometry to analyze and identify the insights of both Pcov and PSE of LoRa networks respect to several essential parameters. Particularly, the novelties and contributions of this manuscript can be summarized as follows.

- A recent definition of the coverage probability is yielded which is able to take into account the correlation between noise and interference at the receiver.
- The approximated but tractable, closed-form expressions of both Pcov and PSE under Nakagami-$m$ fading are provided.
- The trends of the Pcov are investigated based on the proposed mathematical frameworks instead of numerical computations. Particularly, the Pcov is a monotonic decreasing function with convex property respect to the average number of EDs; the impact of the transmit power, on the contrary, is totally opposite. In fact, Pcov is a concave function with monotonic increasing property respect to the transmit power. As for the transmission bandwidth and the network radius, Pcov is a unimodal function respect to the transmission bandwidth and is a monotonic decreasing function respect to the network radius. In addition, the optimal value of the bandwidth that maximizes the Pcov is computed either in closed-form or semi closed-form expressions. To the best of authors' knowledge, these findings are novel especially the impact of the transmission bandwidth.
- As for the PSE, its insights respect to the average number of EDs, the transmit power, the transmission bandwidth and the network radius are also identified. We prove that PSE has identical behaviors with Pcov if the transmit power, network radius and transmission bandwidth are considered. However, the trends of PSE respect to the average number of ED totally disagree with Pcov as it either monotonically increases with concave property or is a unimodal function and changes from concave to convex relying on the transmit power. Furthermore, the insights of the optimal value of the average number of EDs are also investigated as a function of the transmit power, network radius and the path-loss exponent, respectively.
- The trends of Pcov and PSE respect to both the transmit power and the average number of EDs simultaneously are unveiled too. It shows that it always exists a pair of the transmit power and the average number of EDs that maximizes the PSE while the Pcov is simply a concave function of these variables.

The rest of this paper is organized as follows. In Section II, the considered system model is presented. In Section III, both the exact and approximated frameworks of PSE and Pcov are derived and the performances of both metrics respect to various important parameters are investigated in Section IV. In Section V, Monte Carlo simulations are supplied to clarify the correctness of our framework. Finally, Section VI concludes the paper.

TABLE I: Main notations and mathematical symbols/shorthand
$\delta = 2/\beta$, $\mathcal{A} = R^{-2}\left(K_0/\theta\right)^{-\delta}$, $\mathcal{C} = R^{\beta}\left(K_0/\theta\right)$, $\mathcal{D} = \mathcal{A}\mathcal{G}$, $\mathcal{G} = \lambda^{\mathcal{A}}\pi R^2 = \rho_A \overline{N}$, $\mathcal{B} = \sigma^2\gamma_{\mathrm{D}}/P_{\mathrm{tx}}$, $\mathcal{F} = m\theta$, $\widetilde{\mathcal{A}} = R^{-2}(K_0/\mathcal{F})^{-\delta}$, $\widetilde{\mathcal{C}} = R^{-\beta}\mathcal{F}/K_0$, $\widetilde{\mathcal{D}} = \widetilde{\mathcal{A}}\mathcal{G}$, $\mathcal{T}_x\left(t\right)$, $x \in \{0,1,2\}$, is an auxiliary function;
$\phi_x$, $x \in \{1,\ldots,11\}$, is shorthand.

| Symbol | Definition |
|---|---|
| $\mathbb{E}\left\{.\right\}$, $\Pr\left(.\right)$ | Expectation and probability operators |
| $\Gamma\left(.\right)$, $\gamma\left(.,.\right)$ | Gamma and incomplete lower gamma functions |
| $\exp\left(.\right)$, $\log\left(.\right)$ | Exponential and natural logarithm functions |
| $F_X\left(x\right)$, $f_X\left(x\right)$ | Cumulative distribution function and probability density function of RV $X$ |
| $\mathbf{1}\left(x\right)$, $\max\left\{.\right\}$ | Indicator and maximum function |
| $\dot{f}\left(x\right) = df(x)/dx$ | First-order derivative of $f$ respect to $x$ |
| $\ddot{f}\left(x\right) = d^2f(x)/dx^2$ | Second-order derivative of $f$ respect to $x$ |
| $\partial f/\partial x$ | Partial derivative of function $f$ respect to $x$ |
| $h_o$, $h_o^2$ | Fading coefficient and channel gain from ED $o$ to gateway |
| $r_o$, $L_o$ | Distance and path-loss from ED $o$ to gateway |
| Det$\{X\}$, $R$ | The determinant of $X$ matrix and network radius |
| $H_X\left(x,y\right)$ | The Hessian matrix of function $X$ with variables $x$ and $y$ |
| $\lambda$, $\lambda^{\mathcal{A}}$, $\overline{N}$ | The density, active density and average number of EDs |
| $\beta$, $K_0$, $\sigma^2$ | The path-loss exponent, path-loss constant and noise variance |
| $P_{\mathrm{tx}}$ | The transmit power of each ED |
| SF, CR, $L_{\mathrm{pac}}$ | Spreading factor, coding rate and packet length |
| $T_{\mathrm{in}}$, NF, BW | Average packet inter-arrival time, noise figure and bandwidth |
| $m$, $\theta$, $f_c$ | Shape and scale parameters of Gamma distribution, carrier frequency |
| $\Psi^{\mathcal{A}}$, $\Omega$ | Set of active ED and scaling factor of Nakagami-$m$ fading |
| $\gamma_{\mathrm{I}}$, $\gamma_{\mathrm{D}}$ | Rejection threshold and QoS threshold |
| SNR, SIR | Signal-to-noise ratio and signal-to-interference ratio |
| Pcov $\left(\gamma_{\mathrm{D}}\right)$, $\widetilde{\mathrm{Pcov}}\left(\gamma_{\mathrm{D}}\right)$ | Exact and Approximation of the coverage probability |
| PSE $\left(\gamma_{\mathrm{D}}\right)$, $\widetilde{\mathrm{PSE}}\left(\gamma_{\mathrm{D}}\right)$ | Exact and Approximation of the potential spectral efficiency |

## II. System Model

### A. LoRa Networks Modeling

Considering an uplink LoRa networks with single gateway locates at the origin of the coordinate system and the EDs which are randomly distributed in the considered region, $\mathcal{Q}$, around the gateway. We assume that the EDs are modelled according to an inhomogeneous Poisson point process (PPP), $\Psi$, with intensity function $\lambda > 0$ in $\mathcal{Q}$ and 0 otherwise. For simplicity, assuming that the considered region, $\mathcal{Q}$, is a disc with radius, $R$, from the gateway. Consequently, the average number of EDs denoted by $\overline{N}$, is computed as $\overline{N} = \lambda\pi R^2$. In this work, we assume that interference from other LPWAN technologies which operate at the same industrial, scientific and medical (ISM) band are not taken into account as well since we consider only the LoRa networks [5].

### B. Channel Modelling

Let us consider a generic signal from an arbitrary ED to the gateway, it is impaired by both the small-scale fading and the large-scale path-loss. It should be emphasized that the impact of the shadowing is implicitly studied by modifying the density of the EDs [12].

*1) Small-scale fading:* Let us denote $h_o$, is the small-scale fading from an arbitrary node $o$ to the gateway which follows by Nakagami-$m$ fading with severity $m \geq 1/2$, and

scaling factor, $\Omega$. The channel gain, $h_o^2$, as a result, is followed Gamma distribution with corresponding shape and scale parameters, $m$ and $\theta = \frac{m}{\Omega}$, respectively. It is obvious that Nakagami-$m$ fading is one of the most general fading channel which can be turned into other well-known fading distribution by properly setting its severity parameter, e.g., $m = 1$, is Rayleigh fading and $m = 1/2$, is the single-sided Gaussian distribution. In addition, we assume that time is slotted and the fading remains constant during one time-slot and changes between time-slot.

*2) Large-scale path-loss:* Let us consider a transmission link from a generic node $o$ to the gateway, the large-scale path-loss is formulated as

$$L_o = l\left(r_o\right) = K_0 r_o^{\beta}. \tag{1}$$

Here $r_o$ is the distance from the ED $o$ to the gateway; $\beta > 2$ and $K_0 = \left(\frac{4\pi f_c}{c}\right)^2$ are the path-loss exponent and the path-loss constant, respectively. Here, $f_c$ is the carrier frequency and $c = 3 \times 10^8$ (in meter per second) is the speed of light.

### C. Signal-to-Interference Ratio (SIR) and Signal-to-Noise Ratio (SNR)

*1) Signal-to-Interference Ratio (SIR):* Under the considered networks, the signal-to-interference ratio (SIR) from an arbitrary node to the gateway, SIR, is formulated as

$$\text{SIR} = \frac{P_{\text{tx}} S_0}{P_{\text{tx}} I_{\text{S}}} = \frac{P_{\text{tx}} h_0^2 / L_0}{P_{\text{tx}} \sum\limits_{i \in \Psi^{\mathcal{A}} \setminus (0)} \frac{h_i^2}{L_i}} \tag{2}$$

where $P_{\text{tx}}$ is the transmit power of end-devices; $S_0$ is the signals from the ED of interest to the gateway; $I_{\text{S}}$ is the aggregate interference from all active EDs except for the desired ED. $h_0^2$, $h_i^2$ are the channel gain from desired ED and interferer $i$ to the gateway; and $L_0$, $L_i$ are the large-scale path-loss from the ED of interest and interferer $i$ to the gateway. $\Psi^{\mathcal{A}} \setminus (0)$ is the set of active EDs except for the desired ED and follows an homogeneous PPP which density $\lambda^{\mathcal{A}} = p_A \lambda$ in $\mathcal{Q}$. Here, $p_A = \frac{1}{T_{\text{in}}} \frac{L_{\text{pac}}}{R_{\text{bit}}}$ being active probability; $T_{\text{in}}$, $L_{\text{pac}}$ are the average packet inter arrival time and the packet length, respectively. The length of the packet assumes to be fixed and $R_{\text{bit}}$ is bit rate and computes as $R_{\text{bit}} = \text{SF}\frac{\text{BW}}{2^{\text{SF}}}\text{CR}$ [3]; SF, CR and BW are the spreading factor, coding rate and transmission bandwidth, respectively. Table I summarizes all notations/symbols are used in the paper.

*2) Signal-to-Noise Ratio (SNR):* Let us denote SNR is the signal-to-noise ratio (SNR) of an arbitrary node to the gateway and is formulated as

$$\text{SNR} = \frac{P_{\text{tx}} S_0}{\sigma^2}, \tag{3}$$

where $\sigma^2 = 10^{(-174+\text{NF}+10\log_{10}\text{BW})/10}$ [5] is the noise variance of AWGN noise; NF is the noise figure (in dBm) at receiver and $\log_{10}(.)$ is the logarithm base 10 function.

## III. Performance Analysis

### A. Performance Metrics

In this manuscript, we are interested in investigating the performance of LoRa networks from two perspectives, namely, from the end-devices and from the whole networks point of view. From the viewpoint of EDs, the coverage probability (Pcov) is selected while the potential spectral efficiency (PSE) is chosen from the viewpoint of the whole networks.

*1) Coverage Probability:* Considering a generic ED, the coverage probability denoted by $\text{Pcov}\left(\gamma_{\text{D}}\right)$, refers to the probability that both SIR and SNR are greater than the pre-defined thresholds and is formulated as follows [13]:

$$\text{Pcov}\left(\gamma_{\text{D}}\right) = \Pr\left\{\text{SIR} \geq \gamma_{\text{I}}, \text{SNR} \geq \gamma_{\text{D}}\right\}, \tag{4}$$

where $\Pr\{.\}$ is the probability operator; $\gamma_{\text{D}}$ is a given quality-of-services threshold and relying on the spreading factor [3]; $\gamma_{\text{I}}$ is the rejection threshold. In LoRa, the receiver can successfully decode its desired signal provided that no other signals with the same SF is greater than 6 dB, i.e., $\gamma_{\text{I}} = 6$ dB [3].

By direct inspection the Pcov definition in (4), it is no doubt that it has taken into account the correlation between the interference and background noise. The work in [5], [6], on the other hand, were totally omitted this relationship. Comparing with the definition based on signal-to-interference-plus-noise ratio (SINR) in [9]. The proposed one can be seen as an approximated but more tractable, moreover, it also allows identifying the impact of several important metrics by utilizing the mathematical framework instead of numerical results like in [9].

*2) Potential Spectral Efficiency:* The potential spectral efficiency in (bit/s/m$^2$) measures the network information rate per unit area which corresponds to the minimum QoS requirement and is formulated as follows [12]:

$$\text{PSE}\left(\gamma_{\text{D}}\right) = \lambda^{\mathcal{A}} \text{BW} \log_2\left(1+\gamma_{\text{D}}\right) \text{Pcov}\left(\gamma_{\text{D}}\right). \tag{5}$$

From (4) and (5), it is evident that in order to compute the PSE and Pcov, the distribution of both the intended signal and the aggregate interference are required. In LoRa, a number of concurrent transmissions are limited due to the strict constraint of the duty cycle; as a consequence, it typically approximates the aggregate interference by the dominant interference [5], [6]. Thus, the approximated SIR is given as $\text{SIR} = \frac{P_{\text{tx}} S_0}{P_{\text{tx}} I_{\text{S}}} \approx \frac{P_{\text{tx}} S_0}{P_{\text{tx}} I_{\text{M}}}$, where $I_{\text{M}} = \max\limits_{i \in \Psi^{\mathcal{A}} \setminus (0)} \left(h_i^2 / L_i\right)$ is the strongest interferer. Three following Lemmas are essential to calculate the performance of both PSE and Pcov and are given as follow.

*Lemma 1:* Let us denote $\gamma\left(.,.\right)$ is the lower incomplete gamma function and $\delta = 2/\beta$ then the cumulative distribution function (CDF), $F_{S_0}\left(x\right)$, and probability density function (PDF),

$f_{S_0}(x)$, of the intended signal are provided as follows

$$\begin{aligned} F_{S_0}(x) &= (\Gamma(m))^{-1}\left(\gamma(m,\mathcal{C}x) - \mathcal{A}x^{-\delta}\gamma(\delta+m,\mathcal{C}x)\right), \\ f_{S_0}(x) &= (\delta\mathcal{A}/\Gamma(m))\, x^{-\delta-1}\gamma(\delta+m,\mathcal{C}x), \end{aligned} \tag{6}$$

where $\mathcal{A} = \frac{1}{R^2}\left(\frac{K_0}{\theta}\right)^{-\delta}$; $\mathcal{C} = R^{\beta}\left(\frac{K_0}{\theta}\right)$ and $\Gamma(.)$ is the Gamma function.

*Proof:* The proof begins with the definition of the CDF follow by substituting the distribution of $h_0^2$ and $r_0^{\beta}$. Mathematical speaking, we have following:

$$\begin{aligned} F_{S_0}(x) &= \Pr\left\{\frac{h_0^2}{K_0 r_0^{\beta}} < x\right\} = \Pr\left\{h_0^2 < xK_0 r_0^{\beta}\right\} \\ &\overset{(a)}{=} \frac{1}{\Gamma(m)}\frac{2}{R^2}\frac{1}{\beta}\int_{t=0}^{R^{\beta}} \gamma\left(m, \frac{xK_0 t}{\theta}\right) t^{\delta-1} dt \\ &\overset{(b)}{=} \gamma(m,\mathcal{C}x)/\Gamma(m) - \mathcal{A}x^{-\delta}\gamma(\delta+m,\mathcal{C}x)/\Gamma(m), \end{aligned} \tag{7}$$

where $(a)$ is obtained by applying the CDF of the small-scale fading, $h_0^2$, and the PDF of the distance from the desired ED to the gateway, $r_0$; follow by changing the variable, $t = r_0^{\beta}$; $(b)$ is attained from [14]. The PDF is effortlessly derived by taking the first-order derivative of $F_{S_0}(x)$ respect to $x$ as $f_{S_0}(x) = \dot{F}_{S_0}(x) = \frac{dF_{S_0}(x)}{dx}$ and is shown in (6), we conclude the proof here. □

*Lemma 2:* Let us define $\mathcal{G} = \lambda^{\mathcal{A}}\pi R^2 = \rho_A \overline{N}$ is the number of active EDs then the cumulative distribution function of the strongest interferer is provided as

$$F_{I_{\mathrm{M}}}(x) = \exp\left(-\mathcal{D}x^{-\delta}\frac{\gamma(\delta+m,\mathcal{C}x)}{\Gamma(m)} - \mathcal{G} + \mathcal{G}\frac{\gamma(m,\mathcal{C}x)}{\Gamma(m)}\right), \tag{8}$$

where $\mathcal{D} = \mathcal{A}\mathcal{G}$ and $\exp(.)$ is the exponential function.

*Proof:* The proof is obtained by utilizing the order statistics theorem. In particular, from order statistics, the CDF of the maximum of $i \in \mathbb{N}$, independent and identical distributed (i.i.d.) random variables (RVs) with CDF $F_I(x)$ is calculated as $F_{I_{\mathrm{M}}}(x) = (F_I(x))^i$. In addition, under the considered system, the number of active interferer is followed Poisson distribution with mean $\mathcal{G}$. As a result, the CDF of the dominant interferer is given as

$$\begin{aligned} F_{I_{\mathrm{M}}}(x) &\overset{(a)}{=} \exp(-\mathcal{G})\sum_{i=0}^{\infty}\left[\frac{\gamma(m,\mathcal{C}x)}{\Gamma(m)} - \frac{\mathcal{A}}{x^{\delta}}\frac{\gamma(\delta+m,\mathcal{C}x)}{\Gamma(m)}\right]^i \frac{(\mathcal{G})^i}{i!} \\ &\overset{(b)}{=} \exp\left(-\mathcal{D}x^{-\delta}\frac{\gamma(\delta+m,\mathcal{C}x)}{\Gamma(m)} - \mathcal{G} + \mathcal{G}\frac{\gamma(m,\mathcal{C}x)}{\Gamma(m)}\right). \end{aligned} \tag{9}$$

Here $(a)$ is attained by substituting the CDF of an arbitrary interferer and taking the average over number of interferer; $(b)$ is held by using the definition of the exponential function, $\sum_{i=0}^{\infty}\frac{x^i}{i!} = \exp(x)$ and $\mathcal{D} = \mathcal{A}\mathcal{G}$. We complete the proof here. □

*Lemma 3:* Let us denote $\widetilde{S_0} \approx S_0 = \frac{\mathbb{E}\{h_0^2\}}{L_0}$, $\widetilde{I_{\mathrm{M}k}} \approx I_{\mathrm{M}} = \max\limits_{i \in \Psi^{\mathcal{A}} \setminus (0)} \frac{\mathbb{E}\{h_i^2\}}{L_i}$ are the approximated desired signal and dominant interferer, respectively. Then, the PDF of the signals of interest and the CDF of the strongest interferer are computed as

$$\begin{aligned} F_{\widetilde{S_0}}(x) =& \Pr\left\{\frac{\mathbb{E}\{h_0^2\}}{K_0 r_0^{\beta}} \leq x\right\} = \left(1 - \widetilde{\mathcal{A}} x^{-\delta}\right) \mathbf{1}\left(x - \widetilde{\mathcal{C}}\right), \\ f_{\widetilde{S_0}}(x) =& \delta \widetilde{\mathcal{A}} x^{-\delta-1} \mathbf{1}\left(x - \widetilde{\mathcal{C}}\right) \\ F_{\widetilde{I_{\mathrm{M}}}}(x) =& \exp\left(-\mathcal{G}\mathbf{1}\left(\widetilde{\mathcal{C}} - x\right)\right) \exp\left(-\widetilde{\mathcal{D}} x^{-\delta} \mathbf{1}\left(x - \widetilde{\mathcal{C}}\right)\right), \end{aligned} \tag{10}$$

where $\widetilde{\mathcal{A}} = \frac{1}{R^2}\left(\frac{K_0}{\mathcal{F}}\right)^{-\delta}$, $\widetilde{\mathcal{C}} = \frac{\mathcal{F}}{R^{\beta} K_0}$, $\widetilde{\mathcal{D}} = \widetilde{\mathcal{A}}\mathcal{G}$; $\mathcal{F} = m\theta$; $\mathbb{E}\{.\}$ is the mean operator and $\mathbf{1}(x)$ is the indicator function which is equal to 1 if $x > 0$ and 0 for otherwise.

*Proof:* The proof is straightforwardly derived by following the same steps as Lemmas 1 and 2. □

Lemmas 1 and 2 provide the statistics of the intended signal and the strongest interferer in the exact frameworks while Lemma 3 gives the approximated one. The core reason of using approximated frameworks is that the closed-form expression of the Pcov can only be obtained by the approximated framework, the exact one, on the other hand, is not able to attain even the simplest case, i.e., Rayleigh fading or $m = 1$, is taken into consideration, i.e., equation (11). Moreover, it is emphasized that the trends of both Pcov and PSE can merely be drawn based on the rigorous mathematical frameworks providing that the approximated signals are yielded.

### *B. Performance Analysis*

From Lemmas 1 and 2, the coverage probability formulated in (4) is computed as follows

$$\begin{aligned} \mathrm{Pcov}(\gamma_{\mathrm{D}}) =& \frac{\delta \mathcal{A}}{\Gamma(m)} \exp(-\mathcal{G}) \int_{x=\mathcal{B}}^{\infty} x^{-\delta-1} \gamma(\delta + m, \mathcal{C}x) \\ & \times \exp\left(-\mathcal{D} x^{-\delta} (\gamma_{\mathrm{I}})^{\delta} \frac{\gamma\left(\delta + m, x\mathcal{C}(\gamma_{\mathrm{I}})^{-1}\right)}{\Gamma(m)} + \mathcal{G}\frac{\gamma\left(m, x\mathcal{C}(\gamma_{\mathrm{I}})^{-1}\right)}{\Gamma(m)}\right) dx, \end{aligned} \tag{11}$$

*Proof:* Equation (11) is easily derived from the definition of Pcov in (4) as $\mathrm{Pcov}(\gamma_{\mathrm{D}}) = \Pr\{S_0/\gamma_{\mathrm{I}} \geq I_{\mathrm{M}}, S_0 \geq \mathcal{B}\} = \int_{x=\mathcal{B}}^{\infty} F_{I_{\mathrm{M}}}(x/\gamma_{\mathrm{I}}) f_{S_0}(x)\, dx$ and $\mathcal{B} = \sigma^2 \gamma_{\mathrm{D}} / P_{\mathrm{tx}}$. □

By direct examination (11), it is obvious that the integration is not able to compute in closed-form expression even with the simplest case, $m = 1$ (Rayleigh fading) or in the high transmit power regime, i.e., $P_{\mathrm{tx}} \to \infty \Rightarrow \mathcal{B} \to 0$, owing to the generality of the path-loss exponent as well as the composition function of the lower incomplete gamma function and the exponential function. As a result, we propose a simple but tractable approximation framework in order to not only obtain the closed-form expression but also derive the trends of Pcov respect to some essential parameters based on the rigorous frameworks. The accuracy of the

proposed approximation framework versus its counterpart are extensively studied in Section V. Considering the small-scale fading remains constant over a lengthy of time, consequently, following approximation can be applied: $h_w^2 \approx \mathbb{E}\{h_w^2\}$, $w \in \{0, i\}$, then the approximated Pcov is provided in Proposition 1 as follows

*Proposition 1:* Let us denote $\widetilde{\text{Pcov}}(\gamma_{\text{D}})$ is the approximated of $\text{Pcov}(\gamma_{\text{D}})$, it is formulated and computed as

$$\widetilde{\text{Pcov}}(\gamma_{\text{D}}) \approx \Pr\left\{\widetilde{S}_0/\widetilde{I_{\text{M}}} \geq \gamma_{\text{I}}, P_{\text{tx}}\widetilde{S}_0/\sigma^2 \geq \gamma_{\text{D}}\right\} = (\mathcal{G})^{-1}(\gamma_{\text{I}})^{-\delta}\Bigg(1 - \exp\Bigg(-(\gamma_{\text{I}})^{\delta}\widetilde{\mathcal{D}} \times \left(\max\left\{\mathcal{B}, \gamma_{\text{I}}\widetilde{\mathcal{C}}\right\}\right)^{-\delta}\Bigg)\Bigg) + \widetilde{\mathcal{A}}\exp(-\mathcal{G})\left(\left(\max\left\{\widetilde{\mathcal{C}}, \mathcal{B}\right\}\right)^{-\delta} - \left(\gamma_{\text{I}}\widetilde{\mathcal{C}}\right)^{-\delta}\right)\mathbf{1}\left(\gamma_{\text{I}}\widetilde{\mathcal{C}} - \mathcal{B}\right), \quad (12)$$

where $\max\{.,.\}$ is the maximum function.

*Proof:* See Appendix I. □

Having the Pcov in hand, we are now able to compute the PSE by substituting (11) and (12) into (5). It is worth noting that if (12) is yielded then we have the approximated PSE denoted by $\widetilde{\text{PSE}}(\gamma_{\text{D}})$ instead of the exact one. In the sequel, the insights of both Pcov and PSE will be studied based on the approximated frameworks.

## IV. Performance Trends

The goal of this section is to investigate the impact of some vital parameters, i.e., the average number of EDs, the transmit power, the network radius and the transmission bandwidth, on the performance of the considered LoRa networks. In particular, based on the approximation framework in equations (12) and (5), we unveil the insights of both Pcov and PSE under the rigorous mathematical framework which is almost impossible to get the same conclusions providing that (11) is considered.

For clarification, in the following, let us denote the parameter of interest as follows $\omega = \overline{N}$, $\xi = P_{\text{tx}}$, $\varsigma = \text{BW}$ and $\varpi = R$. Without loss of generality, only the parameter of interest, e.g., $\omega, \xi, \varsigma$ and $\varpi$, is explicitly shown in the framework of both Pcov and PSE, thus, it implicitly means that other parameters are constant and for ease of notation, following shorthand are introduced $\widetilde{\text{Pcov}}(\gamma_{\text{D}}) = \widetilde{\mathcal{P}}(x)$; $\widetilde{\text{PSE}} = \widetilde{\mathcal{S}}(x)$, $x \in \{\omega, \xi, \varsigma, \varpi\}$. For example, $\widetilde{\mathcal{P}}(\xi)$ means the coverage probability is solely a function of the transmit power and other parameters are fixed.

### A. Coverage Probability

Let us first investigate the behaviors of Pcov respect to the average number of EDs, $\overline{N}$, which is provided in Proposition 2.

*Proposition 2:* Let us consider $\omega = \overline{N}$, the followings are held: i) $\widetilde{\mathcal{P}}(\omega)$ has the convexity, monotonic decreasing properties respect to $\omega$; ii) $\widetilde{\mathcal{P}}(\omega \to +\infty) = 0$; and iii) $\widetilde{\mathcal{P}}(\omega \to 0) =$

$\widetilde{\mathcal{A}}\left[\left(\max\left\{\mathcal{B},\gamma_{\mathrm{I}}\widetilde{\mathcal{C}}\right\}\right)^{-\delta}+\left(\left(\max\left\{\widetilde{\mathcal{C}},\mathcal{B}\right\}\right)^{-\delta}-\left(\gamma_{\mathrm{I}}\widetilde{\mathcal{C}}\right)^{-\delta}\right)\mathbf{1}\left(\gamma_{\mathrm{I}}\widetilde{\mathcal{C}}-\mathcal{B}\right)\right]$.

*Proof:* See Appendix II. □

*Remark 1:* By direct inspection (11), we can also draw the same conclusion that Pcov is monotonically decreasing to zero at

$$\begin{aligned}\mathrm{Pcov}\left(\gamma_{\mathrm{D}}\right)\overset{\overline{N}\to 0}{=}\mathcal{P}\left(\omega\to 0\right)&=\left(\delta\mathcal{A}/\Gamma\left(m\right)\right)\int_{x=\mathcal{B}}^{\infty}x^{-\delta-1}\gamma\left(\delta+m,\mathcal{C}x\right)dx\\&=1-\left(\Gamma\left(m\right)\right)^{-1}\left(\gamma\left(m,\mathcal{B}\mathcal{C}\right)-\mathcal{A}(\mathcal{B})^{-\delta}\gamma\left(\delta+m,\mathcal{B}\mathcal{C}\right)\right).\end{aligned}\tag{13}$$

The second-order property of Pcov, however, is not able to immediately derive from the exact framework, i.e., equation (11). As a result, our findings in Proposition 2 are not trivial.

*Remark 2:* It is also interested in stating that the asymptotic of Pcov when $\overline{N}\to 0$, i.e., $\mathcal{P}\left(\omega\to 0\right)$, can be intuitively derived from (4) if the considered networks is noise-limited. Mathematical speaking, we have

$$\mathrm{Pcov}\left(\gamma_{\mathrm{D}}\right)=\Pr\left\{\mathrm{SNR}=\frac{P_{\mathrm{tx}}S_0}{\sigma^2}\geq\gamma_{\mathrm{D}}\right\}\overset{(a)}{=}\overline{F}_{S_0}\left(\mathcal{B}\right).\tag{14}$$

Here $\overline{F}_X\left(x\right)$ is the complementary cumulative distribution function (CCDF) of random variable $X$, i.e., $\overline{F}_X\left(x\right)=1-F_X\left(x\right)$, and $(a)$ is held by using the result of (7).

*Remark 3:* Looking at the framework of $\widetilde{\mathcal{P}}\left(\omega\to 0\right)$, in general, the upper bound of Pcov when $\omega\to 0$ is not equal to 1. It is facile to explain that although the system is no longer interference-limited, the impact of the fading and noise on the Pcov, on the other hand, are not non-negligible. Nevertheless, if keep increasing the transmit power that $\mathcal{B}\to 0$, then Pcov approaches 1 as expected.

In the sequel, the impact of the transmit power on the performance of Pcov is provided by following proposition.

*Proposition 3:* Let us consider $\xi=P_{\mathrm{tx}}$, the followings are true: i) $\widetilde{\mathcal{P}}\left(\xi\right)$ monotonically increases and has concavity property with $\xi$; ii) $\widetilde{\mathcal{P}}\left(\xi\to+\infty\right)=\left(\mathcal{G}\right)^{-1}\left(\gamma_{\mathrm{I}}\right)^{-\delta}\left(1-\exp\left(-\mathcal{G}\right)\right)+\exp\left(-\mathcal{G}\right)\left(1-\left(\gamma_{\mathrm{I}}\right)^{-\delta}\right)$; iii) $\widetilde{\mathcal{P}}\left(\xi\to 0\right)=0$.

*Proof:* See Appendix III. □

*Remark 4:* It is apparent that the Pcov's behaviors respect to $\xi=P_{\mathrm{tx}}$, are not able to derive from (11) due to the extremely high complexity of the function inside the integration. On the contrary, it is not a problem if we inspect the definition of Pcov provided in (4). However, for the second-order property, it is impossible to proof the trends by direct inspection either (11) or (4). Hence, once again, our findings are valuable and also confirm the necessity of the closed-form expression of the Pcov.

*Remark 5:* From Proposition 3, we observe that there is an upper bound of Pcov when $P_{\mathrm{tx}}\to\infty$ and this bound, in general, does not approach one. Indeed, it can only go to one

providing that two following conditions, i.e., $P_{\text{tx}} \to \infty$ and $\mathcal{G} \to 0$, are concurrently satisfied and this coincides with findings in Remark 3.

Propositions 2 and 3 investigate the properties of Pcov separately. In the sequel, the impact of both the average number of EDs, $\overline{N}$, and the transmit power, $P_{\text{tx}}$, on the coverage probability are simultaneously addressed.

*Proposition 4:* Let us define $\omega = \overline{N}$ and $\xi = P_{\text{tx}}$, the Pcov as a function of both $\omega$ and $\xi$, $\widetilde{\mathcal{P}}(\omega, \xi)$, is a concave function.

*Proof:* Let us explicitly represent Pcov respect to both $\omega$ and $\xi$ as follows

$$\widetilde{\mathcal{P}}(\omega,\xi) = (\gamma_{\text{I}})^{-\delta} (\mathcal{G}(\omega))^{-1} \left(1 - \exp\left(-\widetilde{\mathcal{A}}\mathcal{G}(\omega)(\gamma_{\text{I}})^{\delta}\left(\max\left\{\mathcal{B}(\xi), \gamma_{\text{I}}\widetilde{\mathcal{C}}\right\}^{-\delta}\right)\right)\right)$$
$$+ \widetilde{\mathcal{A}} \exp(-\mathcal{G}(\omega)) \left(\max\left\{\mathcal{B}(\xi), \widetilde{\mathcal{C}}\right\}^{-\delta} - \left(\gamma_{\text{I}}\widetilde{\mathcal{C}}\right)^{-\delta}\right) \mathbf{1}\left(\gamma_{\text{I}}\widetilde{\mathcal{C}} - \mathcal{B}(\xi)\right). \tag{15}$$

To find out the concavity property of a given function, the determinant of the Hessian matrix of $\widetilde{\mathcal{P}}(\omega, \xi)$ is computed as

$$H_{\widetilde{\mathcal{P}}}(\omega,\xi) = \begin{bmatrix} \frac{\partial^2\widetilde{\mathcal{P}}(\omega,\xi)}{\partial^2\omega} & \frac{\partial^2\widetilde{\mathcal{P}}(\omega,\xi)}{\partial\omega\partial\xi} \\ \frac{\partial^2\widetilde{\mathcal{P}}(\omega,\xi)}{\partial\xi\partial\omega} & \frac{\partial^2\widetilde{\mathcal{P}}(\omega,\xi)}{\partial^2\xi} \end{bmatrix}$$
$$\text{Det}\left\{H_{\widetilde{\mathcal{P}}}(\omega,\xi)\right\} = \frac{\partial^2\widetilde{\mathcal{P}}(\omega,\xi)}{\partial^2\omega}\frac{\partial^2\widetilde{\mathcal{P}}(\omega,\xi)}{\partial^2\xi} - \left(\frac{\partial^2\widetilde{\mathcal{P}}(\omega,\xi)}{\partial\omega\partial\xi}\right)^2 \leq 0. \tag{16}$$

Here $H_X(a,b)$ is the Hessian matrix of function $X$ respect to variables $a, b$; Det$\{X\}$ is the determinant of matrix $X$; $\frac{\partial f}{\partial a}$ is the partial derivative of $f$ respect to variable $a$; (16) is obtained directly by exploiting the outcomes of Propositions 2 and 3 that $\frac{\partial^2\widetilde{\mathcal{P}}(\omega,\xi)}{\partial^2\omega} \geq 0, \forall\omega$ and $\frac{\partial^2\widetilde{\mathcal{P}}(\omega,\xi)}{\partial^2\xi} \leq 0, \forall\xi$. As the determinant of the Hessian matrix is always negative, hence, Pcov is a concave function and we close the proof here. □

*Remark 6:* Proposition 4 means that there always exists a pair of $(\omega, \xi)$ that maximizes the Pcov.

The impact of other equal-important parameters, i.e., the transmission bandwidth and the network radius, are provided by two following Propositions.

*Proposition 5:* Let us define $\varsigma = \text{BW}$, the coverage probability of EDs is a parabola function with concave down property respect to $\varsigma$. Given the value of the transmit power, the optimal value of $\varsigma$ denoted by $\varsigma^*_{\mathcal{P}} = \text{BW}^*$, that maximizes Pcov is computed as follows

$$\varsigma^*_{\mathcal{P}} = \begin{cases} \left[(\gamma_{\text{I}})^{\delta}\widetilde{\mathcal{A}}\phi_8(\phi_9)^{-\delta}(\varsigma_1^*)^{-1}\right]^{\frac{1}{1+\delta}} & P_{\text{tx}} \leq \frac{\phi_7\gamma_{\text{D}}\phi_8}{\gamma_{\text{I}}\widetilde{\mathcal{C}}\varsigma_1^*} \\ \varsigma_2^* & P_{\text{tx}} \in \left(\frac{\phi_7\gamma_{\text{D}}\phi_8}{\gamma_{\text{I}}\widetilde{\mathcal{A}}\varsigma_1^*}, \frac{\phi_7\gamma_{\text{D}}\phi_8}{\delta\widetilde{\mathcal{C}}}\right] \\ \frac{P_{\text{tx}}\widetilde{\mathcal{A}}}{\phi_7\gamma_{\text{D}}} & P_{\text{tx}} > \frac{\phi_7\gamma_{\text{D}}\phi_8}{\delta\widetilde{\mathcal{C}}} \end{cases} \tag{17}$$

where $\phi_7 = 10^{(-174+\text{NF})/10}$; $\phi_8 = \frac{L_{\text{pac}}\overline{N}2^{\text{SF}}}{\text{SF}T_{\text{in}}\text{CR}}$; $\phi_9 = \phi_7\gamma_{\text{D}}/P_{\text{tx}}$; $\varsigma_1^*$ and $\varsigma_2^*$ are the solution of

following equations

$$1-\exp\left(-\varsigma_1^*\right)\left(\varsigma_1^*\left(1+\delta\right)+1\right)=0 \tag{18}$$

$$\widetilde{\mathcal{A}}(\mathcal{B}\left(\varsigma_2^*\right))^{-\delta}\exp\left(-\mathcal{G}\left(\varsigma_2^*\right)\right)\left(\mathcal{G}\left(\varsigma_2^*\right)-\delta\right)+\left(\gamma_{\mathrm{I}}\right)^{-\delta}\left(\mathcal{G}\left(\varsigma_2^*\right)\right)^{-1}$$
$$\times\left[1-\exp\left(-\mathcal{G}\left(\varsigma_2^*\right)\right)\left(1+\mathcal{G}\left(\varsigma_2^*\right)+\left(\mathcal{G}\left(\varsigma_2^*\right)\right)^2\right)\right]=0 \tag{19}$$

*Proof:* See Appendix IV. □

*Remark 7:* It is noted that if the transmit power goes to infinity then $\varsigma_{\mathcal{P}}^*$ approaches infinity too. The Pcov, as a result, is monotonically increasing to one for this case study.

*Remark 8:* To the best of authors' knowledge, none of works in the literature examines the performance of Pcov respect to the transmission bandwidth in LoRa networks; thus, the results reported in Proposition 5 are novel and unique. Moreover, it is, for sure, impossible to have the same conclusions if the exact framework is taken into consideration.

*Remark 9:* It is worth noting that although $\varsigma_{\mathcal{P}}^*$ is computed either in full or semi closed-form expression because $\varsigma_1^*$ and $\varsigma_2^*$ need to be calculated by using numerical methods via some commercial software, e.g., Matlab or Mathematica. However, these values can be effortlessly found, for example, looking at (18), it is quite simple and relies solely on the path-loss exponent, $\beta$, via the term $\delta$.

*Proposition 6:* Let us consider $\varpi=R$, the followings are true: i) $\widetilde{\mathcal{P}}\left(\varpi\right)$ is monotonically decreasing with $\varpi$; ii) $\widetilde{\mathcal{P}}\left(\varpi\to 0\right)=\left(\mathcal{G}\right)^{-1}\left(\gamma_{\mathrm{I}}\right)^{-\delta}\left(1-\exp\left(-\mathcal{G}\right)\right)+\exp\left(-\mathcal{G}\right)\left(1-\left(\gamma_{\mathrm{I}}\right)^{-\delta}\right)$; and iii) $\widetilde{\mathcal{P}}\left(\varpi\to+\infty\right)=0$.

*Proof:* The proof can be derived straightforwardly by computing the first-order derivative of Pcov respect to the network radius as follows

$$\begin{aligned}\widetilde{\mathcal{P}}\left(\varpi\right)=&\left(\mathcal{G}\right)^{-1}\left(\gamma_{\mathrm{I}}\right)^{-\delta}\left(1-\exp\left(-\left(\gamma_{\mathrm{I}}\right)^{\delta}\left(\max\left\{\mathcal{B},\gamma_{\mathrm{I}}\widetilde{\mathcal{C}}\left(\varpi\right)\right\}\right)^{-\delta}\widetilde{\mathcal{A}}\left(\varpi\right)\mathcal{G}\right)\right)\\&+\widetilde{\mathcal{A}}\left(\varpi\right)\exp\left(-\mathcal{G}\right)\left(\left(\max\left\{\widetilde{\mathcal{C}}\left(\varpi\right),\mathcal{B}\right\}\right)^{-\delta}-\left(\gamma_{\mathrm{I}}\widetilde{\mathcal{C}}\left(\varpi\right)\right)^{-\delta}\right)\mathbf{1}\left(\gamma_{\mathrm{I}}\widetilde{\mathcal{C}}\left(\varpi\right)-\mathcal{B}\right)\end{aligned} \tag{20}$$

$$\begin{aligned}\dot{\widetilde{\mathcal{P}}}\left(\varpi\right)=&\dot{\widetilde{\mathcal{A}}}\left(\varpi\right)\left(\mathcal{B}\right)^{-\delta}\exp\left(-\left(\gamma_{\mathrm{I}}\right)^{\delta}\left(\mathcal{B}\right)^{-\delta}\widetilde{\mathcal{A}}\left(\varpi\right)\mathcal{G}\right)\mathbf{1}\left(\mathcal{B}-\gamma_{\mathrm{I}}\widetilde{\mathcal{C}}\left(\varpi\right)\right)\\&+\dot{\widetilde{\mathcal{A}}}\left(\varpi\right)\exp\left(-\mathcal{G}\right)\left(\mathcal{B}\right)^{-\delta}\mathbf{1}\left(\gamma_{\mathrm{I}}\widetilde{\mathcal{C}}\left(\varpi\right)-\mathcal{B}\right)\mathbf{1}\left(\mathcal{B}-\widetilde{\mathcal{C}}\left(\varpi\right)\right)\leq 0,\forall\varpi>0,\end{aligned} \tag{21}$$

where $\widetilde{\mathcal{A}}\left(\varpi\right)=\frac{1}{\varpi^2}\left(\frac{K_0}{\mathcal{F}}\right)^{-\delta}\Rightarrow\dot{\widetilde{\mathcal{A}}}\left(\varpi\right)=-\frac{2}{\varpi^3}\left(\frac{K_0}{\mathcal{F}}\right)^{-\delta}$ and $\widetilde{\mathcal{C}}\left(\varpi\right)=\frac{\mathcal{F}}{\varpi^{\beta}K_0}$. As for the asymptotic performance of Pcov when $\varpi\to 0$, it is not difficult to derive from (20), i.e., $\varpi\to 0\Rightarrow\widetilde{\mathcal{C}}\left(\varpi\right)\to+\infty\Rightarrow\max\left\{\widetilde{\mathcal{C}}\left(\varpi\right),\mathcal{B}\right\}=\widetilde{\mathcal{C}}\left(\varpi\right)$ and we complete the proof here. □

*Remark 10:* It is interested in pointing out that the asymptotic behavior of Pcov when $R\to 0$ is exactly the same as $P_{\mathrm{tx}}\to\infty$. This can be simply explicated by observing that $\max\left\{\mathcal{B},\gamma_{\mathrm{I}}\widetilde{\mathcal{C}}\right\}=\gamma_{\mathrm{I}}\widetilde{\mathcal{C}}$ and $\max\left\{\mathcal{B},\widetilde{\mathcal{C}}\right\}=\widetilde{\mathcal{C}}$ when either $R\to 0$ or $P_{\mathrm{tx}}\to\infty$, hence, it converges to the same mathematical framework and the system narrows to noise-limited scenario.

In next section, the insights of PSE respect to these important parameters are rigorously derived from (12) and (5).

### *B. Potential Spectral Efficiency*

Let us pay our attention to the PSE in (5), the trends of the PSE are also investigated respect to $\overline{N}$, $P_{\text{tx}}$, BW and $R$ similar to the Pcov. However, unlike the Pcov which, to some extend, is able to find out the behavior by direct inspection (11), e.g., respect to $\overline{N}$. The $\widetilde{\text{PSE}}$, on the other hand, is unable to intuitively get the conclusion from (11) owing to the multiplicative factor $\lambda^{\mathcal{A}}\text{BW}\log_2\left(1+\gamma_{\text{D}}\right)$ which depends on $\overline{N}$. The findings in this section, as a result, are not trivial and to the best of our knowledge, they have not been mathematically proved elsewhere too. The separate impact of $\overline{N}$, $P_{\text{tx}}$ are reported in Propositions 7 and 8 while Proposition 9 provide the insights of PSE where $\overline{N}$ and $P_{\text{tx}}$ are taken into account together. Furthermore, the trends of PSE respect to the bandwidth and network radius are shown in Propositions 10 and 11, respectively.

*Proposition 7:* Let us define $\omega = \overline{N}$, the following findings are held: i) The $\widetilde{\text{PSE}}$ is a uni-modal function and attains its maximum at $\omega^* = \left(1+\left(\gamma_{\text{I}}\right)^{-\delta}\left[\widetilde{\mathcal{A}}\left(\left(\max\left\{\widetilde{\mathcal{C}},\mathcal{B}\right\}\right)^{-\delta}-\left(\gamma_{\text{I}}\widetilde{\mathcal{C}}\right)^{-\delta}\right)\right]^{-1}\right)\times\left(p_A\right)^{-1}$; and its inflection point at $\omega^{**} = \left(2+\left(\gamma_{\text{I}}\right)^{-\delta}\left[\widetilde{\mathcal{A}}\left(\left(\max\left\{\widetilde{\mathcal{C}},\mathcal{B}\right\}\right)^{-\delta}-\left(\gamma_{\text{I}}\widetilde{\mathcal{C}}\right)^{-\delta}\right)\right]^{-1}\right)\left(p_A\right)^{-1}$ providing that $\mathcal{B} < \gamma_{\text{I}}\widetilde{\mathcal{C}}$; otherwise, PSE is an increasing function with concavity property; ii) $\widetilde{\mathcal{S}}\left(\omega\to+\infty\right) = \left(\gamma_{\text{I}}\right)^{-\delta}\frac{\text{BW}\log_2(1+\gamma_{\text{D}})}{\pi R^2}$ and iii) $\widetilde{\mathcal{S}}\left(\omega\to 0\right) = 0$.

*Proof:* See Appendix V. □

*Remark 11:* It is re-emphasized that the results reported in Proposition 7 cannot directly take from the exact framework, i.e., (11) and (5). Moreover, we observe that there is a counter benefit between Pcov and PSE respect to the average number of EDs from Propositions 2 and 7. More precisely, Proposition 2 states that increasing $\overline{N}$ will be harmful for the Pcov; the PSE, on the other hand, is on the opposite direction that increases with $\overline{N}$ (to some extent). This contradict behavior will be discussed more detail in Section V.

*Remark 12:* By examination the expressions of $\omega^*$ and $\omega^{**}$, it is apparent that $\omega^{**} > \omega^*$; in addition, two points, generally, are identical, thus, the insights of $\omega^{**}$ (or $\omega^*$) respect to all parameters can be freely obtained from $\omega^*$ (or $\omega^{**}$). In particular, three following Corollaries study the behavior of both $\omega^*$ and $\omega^{**}$ respect to the $P_{\text{tx}}$, the network radius, $R$, and the path-loss exponent, $\beta$, respectively.

*Corollary 1:* By direct inspection the maximum and inflection points of PSE in Proposition 7 as a function of the transmit power, we have following conclusions: Both $\omega^*$ and $\omega^{**}$ are monotonically decreasing respect to the transmit power, $P_{\text{tx}}$, if $\frac{\sigma^2\gamma_{\text{D}}}{\gamma_{\text{I}}\widetilde{\mathcal{C}}} \le P_{\text{tx}} \le \frac{\sigma^2\gamma_{\text{D}}}{\widetilde{\mathcal{C}}}$ and remains constant at $\omega^* = \left(1+\left(\left(\gamma_{\text{I}}\right)^{\delta}-1\right)^{-1}\right)\left(p_A\right)^{-1}$ and $\omega^{**} = \left(2+\left(\left(\gamma_{\text{I}}\right)^{\delta}-1\right)^{-1}\right)\left(p_A\right)^{-1}$ providing that $P_{\text{tx}} > \frac{\sigma^2\gamma_{\text{D}}}{\widetilde{\mathcal{C}}}$.

*Proof:* The proof is directly derived by taking the first-order derivative of $\omega^*$ (or $\omega^{**}$) respect to $\xi = P_{\rm tx}$ as follows

$$\dot{\omega}^*(\xi) = \delta\dot{\mathcal{B}}(\xi)(p_A)^{-1}(\gamma_{\rm I})^{-\delta}\frac{\widetilde{\mathcal{A}}(\mathcal{B}(\xi))^{-\delta-1}}{\left(\widetilde{\mathcal{A}}(\mathcal{B}(\xi))^{-\delta}-\left(\gamma_{\rm I}\widetilde{\mathcal{C}}\right)^{-\delta}\right)^2} \leq 0, \quad \frac{\sigma^2\gamma_{\rm D}}{\gamma_{\rm I}\widetilde{\mathcal{C}}} \leq P_{\rm tx} \leq \frac{\sigma^2\gamma_{\rm D}}{\widetilde{\mathcal{C}}} \tag{22}$$

and $\dot{\omega}^*(\xi) = 0,\ P_{\rm tx} > \frac{\sigma^2\gamma_{\rm D}}{\widetilde{\mathcal{C}}}$; where $\mathcal{B}(\xi) = \frac{\sigma^2\gamma_{\rm D}}{\xi} \Rightarrow \dot{\mathcal{B}}(\xi) = -\frac{\sigma^2\gamma_{\rm D}}{\xi^2}$; and $\omega^* = \left(1+\left((\gamma_{\rm I})^{\delta}-1\right)^{-1}\right)(p_A)^{-1}$ is obtained by simply replacing $\max\left\{\widetilde{\mathcal{C}},\mathcal{B}\right\} = \widetilde{\mathcal{C}}$. It is noted that $\dot{\omega}^*(\xi) = \dot{\omega}^{**}(\xi)$, so we can readily obtain the derivation of $\dot{\omega}^{**}(\xi)$ from (22) and close the proof here. □

*Corollary 2:* By direct inspection the maximum and inflection points of PSE in Proposition 7 respect to the network radius, i.e., $R$, we have following conclusion: $\omega^*$, and $\omega^{**}$ simply increase with the network radius, $R$.

*Proof:* As like Corollary 1, the proof can be obtained via the first-order derivative of both $\omega^*$ and $\omega^{**}$ respect to the network radius, $\varpi = R$, and is given as

$$\dot{\omega}^*(\varpi) = -\frac{(p_A)^{-1}\dot{\widetilde{\mathcal{A}}}(\varpi)(\gamma_{\rm I}\mathcal{B})^{-\delta}}{\left(\widetilde{\mathcal{A}}(\varpi)(\mathcal{B})^{-\delta}-(\gamma_{\rm I})^{-\delta}\right)^2}\mathbf{1}\left(\mathcal{B}-\widetilde{\mathcal{C}}(\varpi)\right)\mathbf{1}\left(\gamma_{\rm I}\widetilde{\mathcal{C}}(\varpi)-\mathcal{B}\right) \geq 0 \tag{23}$$

where $\dot{\widetilde{\mathcal{A}}}(\varpi) = -\frac{2}{\varpi^3}\left(\frac{K_0}{\mathcal{F}}\right)^{-\delta} \leq 0$ and we finish the proof here. □

*Corollary 3:* The maximum and inflection points of PSE in Proposition 7 respect to the path-loss exponent, $\beta$, $\omega^*$ and $\omega^{**}$, monotonically increase with the path-loss exponent $\beta$.

*Proof:* Let us consider the mathematical framework of $\omega^*$ as a function of the path-loss exponent $\beta$ for case $\widetilde{\mathcal{C}} \leq \mathcal{B} \leq \gamma_{\rm I}\widetilde{\mathcal{C}}$ as follows

$$\omega^*(\beta) = 1+\left(\frac{1}{R^2}\left(\frac{\gamma_{\rm I}}{\mathcal{B}}\frac{\mathcal{F}}{K_0}\right)^{\delta(\beta)}-1\right)^{-1} \tag{24}$$

Here $\delta(\beta) = 2/\beta$ and we ignore the constant term $p_A$. Next, taking the first-order derivative of (24) respect to $\beta$, we have

$$\dot{\omega}^*(\beta) = \frac{1}{R^2}\frac{2}{\beta^2}\left(\frac{1}{R^2}\left(\frac{\gamma_{\rm I}}{\mathcal{B}}\frac{\mathcal{F}}{K_0}\right)^{\delta(\beta)}-1\right)^{-2}\left(\frac{\gamma_{\rm I}}{\mathcal{B}}\frac{\mathcal{F}}{K_0}\right)^{\delta(\beta)}\log\left(\frac{\gamma_{\rm I}}{\mathcal{B}}\frac{\mathcal{F}}{K_0}\right) \geq 0. \tag{25}$$

Here, (25) is always true as $\frac{\gamma_{\rm I}}{\mathcal{B}}\frac{\mathcal{B}}{K_0} > 1$ thus $\dot{\omega}^*$ is positive; $\log(.)$ is the natural logarithm function. Next, let us move to the second case where $\widetilde{\mathcal{C}} > \mathcal{B}_k$ and taking the first-order derivative of $\omega^*$ respect to $\beta$, we have following

$$\dot{\omega}^*(\beta) = \frac{2}{\beta^2}\left((\gamma_{\rm I})^{\delta(\beta)}-1\right)^{-2}(\gamma_{\rm I})^{\delta(\beta)}\log(\gamma_{\rm I}) \geq 0. \tag{26}$$

From (25) and (26), we state that both $\omega^*$ and $\omega^{**}$ are monotonically increasing with the path-loss exponent. □

*Remark 13:* From Corollaries 1 and 2, we find out that $\overline{N}^*$ improves when $R$ increases and $P_{\text{tx}}$ decreases. Nonetheless, as proven in Propositions 3 and 6 that reducing the transmit power will decrease the coverage probability; the same statement is held for the network radius that increasing $R$ will obviously reduce the Pcov. Thus, once again, it confirms the contradiction behavior between the Pcov and the PSE respect to $\overline{N}$.

*Proposition 8:* Let us define $\xi = P_{\text{tx}}$, the following findings are true: i) $\widetilde{\mathcal{S}}(\xi)$ monotonically increase with concavity property respect to $\xi$; ii) $\widetilde{\mathcal{S}}(\xi \to +\infty) = \lambda^{\mathcal{A}}\text{BW}\log_2(1+\gamma_{\text{D}}) \times \left((\mathcal{G})^{-1}(\gamma_{\text{I}})^{-\delta}(1-\exp(-\mathcal{G})) + \exp(-\mathcal{G})\left(1-(\gamma_{\text{I}})^{-\delta}\right)\right)$ and iii) $\widetilde{\mathcal{S}}(\xi \to 0) = 0$.

*Proof:* From the definition of the PSE, we have $\widetilde{\mathcal{S}}(\xi) = \lambda^{\mathcal{A}}\text{BW}\log_2(1+\gamma_{\text{D}})\widetilde{\mathcal{P}}(\xi)$. Thus, we directly obtain the findings by using the outcomes from Proposition 3. □

*Remark 14:* By comparing Proposition 3 and 8, it is evident that both Pcov and PSE have the same behavior respect to the transmit power that is a concavity function with monotonic increasing property. Thus, this trend is totally opposite to the scenario versus the average number of EDs.

As the trends of PSE are inverse to the Pcov respect to $\overline{N}$, it, in the contrast, is identical to the Pcov respect to $P_{\text{tx}}$. The question is: what are the behaviors of PSE respect to both $\overline{N}$ and $P_{\text{tx}}$ simultaneously? Is it the same or different of Pcov? The following Proposition is provided to address such questions.

*Proposition 9:* Let us define $\omega = \overline{N}$ and $\xi = P_{\text{tx}}$, followings are true: i) the PSE denoted by $\widetilde{\mathcal{S}}(\omega,\xi)$, is a concave function when $\widetilde{\mathcal{C}} < \mathcal{B}(\xi) < \gamma_{\text{I}}\widetilde{\mathcal{C}}$; ii) there exists an inflection point of $(\omega,\xi)$ that the PSE changes from convex to concave and vice versa when $\mathcal{B}(\xi) \geq \gamma_{\text{I}}\widetilde{\mathcal{C}}$.

*Proof:* See Appendix VI. □

*Remark 15:* From Proposition 9, it is clear that the insight of PSE respect to both $\omega$ and $\xi$ is not identical to the Pcov. Particularly, depending on the transmit power the PSE can be either concave or convex function rather than simply concave like Pcov. Moreover, increasing $\overline{N}$ while fixing $P_{\text{tx}}$ tends to improve the PSE in lieu of reducing the Pcov.

*Proposition 10:* Let us define $\varsigma = \text{BW}$, the potential spectral efficiency is a parabola function with concave down property respect to $\varsigma$. Given a value of the transmit power, the optimal value of $\varsigma$ denoted by $\varsigma^*_{\mathcal{S}} = \text{BW}^*$ which maximizes PSE is computed as follows $\varsigma^*_{\mathcal{S}} = \frac{\phi_8\log_2(1+\gamma_{\text{D}})}{\pi R^2}\varsigma^*_{\mathcal{P}}$ where $\varsigma^*_{\mathcal{P}}$ is provided in (17).

*Proof:* Let us re-write the PSE as a function of the transmission bandwidth, $\varsigma$ = BW, then we have

$$\widetilde{\mathcal{S}}(\varsigma) = \lambda^{\mathcal{A}}\varsigma\log_2(1+\gamma_{\text{D}})\widetilde{\mathcal{P}}(\varsigma) = \frac{\phi_8\log_2(1+\gamma_{\text{D}})}{\pi R^2}\widetilde{\mathcal{P}}(\varsigma). \tag{27}$$

Looking at (27), it is trivial to conclude that PSE has exactly the same behavior as Pcov, hence, we can re-use the outcomes of Proposition 5 and conclude the proof here. □

*Proposition 11:* Let us consider $\varpi = R$, the following is true: i) $\widetilde{\mathcal{S}}(\varpi)$ is monotonically

TABLE II: Setup of parameters [15] (unless otherwise stated)

| Parameters [Unit] | Value |
|---|---|
| $P_{\text{tx}}$ [dBm] | 10 |
| $\overline{N}$ | 4500 |
| SF | 7 |
| CR | 4/5 |
| $\gamma_{\text{D}}$ [dBm] | -6 |
| $L_{\text{pac}}$ [bytes] | 20 |
| $T_{\text{in}}$ [s] | 600 |
| $\beta$ | 2.8 |
| $f_c$ [MHz] | 868 |
| BW [KHz] | 125 |
| $\gamma_{\text{I}}$ [dB] | 6 |
| $R$ [m] | 3000 |
| NF [dBm] | 6 |
| $m$ | 3.5 |
| $\Omega$ | 9.5 |

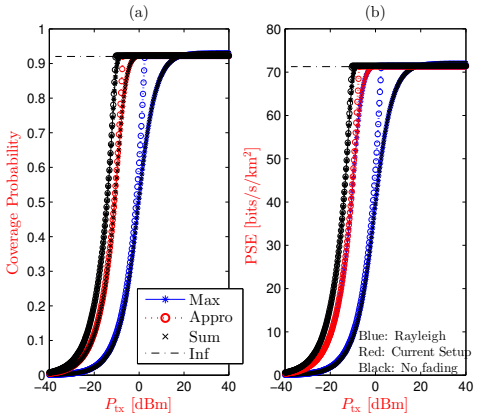


Fig. 1. Coverage probability (a) and potential spectral efficiency (b) versus the transmit power, $P_{\text{tx}}$, with different fading channels, i.e., Rayleigh, current setups and no fading. Here, SF = 8, CR = 0.5, $L_{\text{pac}}$ = 1 byte, $T_{\text{in}}$ = 60 secs, $\gamma_{\text{D}}$ = 6 dBm and $\overline{N}$ = 1500. Solid lines show the exact framework; dot lines show the approximation framework of both Pcov and PSE and are computed by equations (11), (12) and (5), respectively. Markers show Monte-Carlo simulations. Curves with marker "x" correspond to case sum of interference, $I_{\text{S}}$. The curves "Inf" relate to case $P_{\text{tx}} \to \infty$, which are provided in Propositions 3 and 8.

decreasing with $\varpi$.

*Proof:* Let us start formulating the PSE as a function of $\varpi = R$ explicitly as follows

$$\widetilde{\mathcal{S}}\left(\varpi\right) = \frac{\mathcal{G}}{\pi}\log_2\left(1+\gamma_{\text{D}}\right)\varpi^{-2}\widetilde{\mathcal{P}}\left(\varpi\right) = \phi_{11}\varpi^{-2}\widetilde{\mathcal{P}}\left(\varpi\right)$$
$$\dot{\widetilde{\mathcal{S}}}\left(x\right) = \phi_{11}\left[-2\varpi^{-3}\widetilde{\mathcal{P}}\left(\varpi\right) + \varpi^{-2}\dot{\widetilde{\mathcal{P}}}\left(\varpi\right)\right] \leq 0, \forall\varpi \tag{28}$$

where $\phi_{11} = \frac{\mathcal{G}}{\pi}\log_2\left(1+\gamma_{\text{D}}\right)$, we directly obtain the proof by taking the findings in Proposition 6 that $\dot{\widetilde{\mathcal{P}}}\left(\varpi\right) \leq 0$ so we complete the proof here. □

*Remark 16:* From Propositions 10 and 11, it is no doubt that PSE has the same trends as Pcov respect to the bandwidth and network radius.

## V. Numerical Results

In this section, numerical results are provided to confirm the exactitude of our mathematical framework as well as to substantiate our findings in Section IV. A class of IoTs application which applies into smart home, i.e., home security application, is taken into account. Unless otherwise stated, the numerical parameters are provided in Table II.

Fig. 1 verifies the correctness of our proposed approximation versus the exact one via Monte-Carlo simulations with different fading channels, i.e., Rayleigh, setups in Table II and no fading. Particularly, the approximation frameworks of both Pcov and PSE computed by (12) and (5) are close to both the curves based on the dominant interferer computed in (11) and the sum of all interferer, $I_{\text{S}}$ (via Monte-Carlo simulation), especially in low and

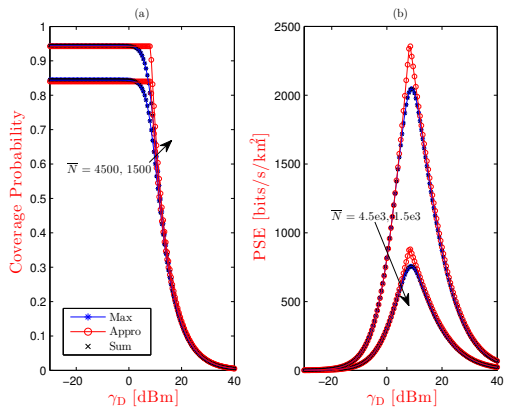


Fig. 2. Coverage probability (a) and potential spectral efficiency (b) versus the QoS threshold, i.e., $\gamma_{\rm D}$. Solid lines show the exact, the approximation framework of both Pcov and PSE and computed by equations (11), (12), (5), respectively. Markers are Monte Carlo simulation. Curves with marker "x" correspond to case sum of interference, $I_{\rm S}$.

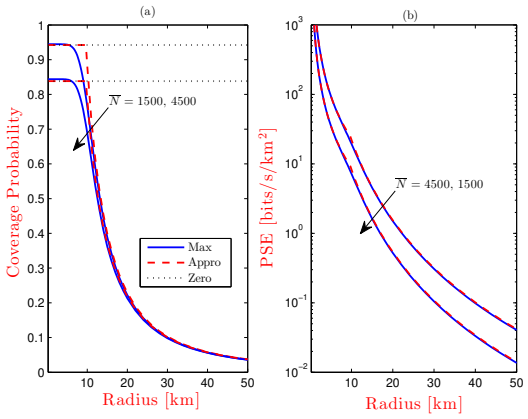


Fig. 3. Coverage probability (a) and potential spectral efficiency (b) versus the network radius, $R$. Solid lines show the exact framework which is computed by (Eqs. (11) and (5)), dash lines show the approximation framework (Eqs. (12), (5)) and the asymptotic framework when $R \to 0$ of Pcov is obtained from *Propositions* 6.

high transmit power regimes. In addition, it is expected that Rayleigh fading performance is the worst since it requires the highest transmit power to reach the maximum; the no fading curves, on the other hand, is the best as around -10 dBm has already achieved the maximum. Moreover, Fig. 1 also confirms the accuracy of our findings in Propositions 3 and 8 that both Pcov and PSE reach its maximum when the transmit power is sufficiently large.

Figure 2 shows the performances of Pcov and PSE as a function of QoS threshold, $\gamma_{\rm D}$. The correctness of the proposed mathematical frameworks are confirmed again by Monte Carlo simulations. It is evident that Pcov based on sum of interferer, $I_{\rm S}$, are indistinguishable with $I_{\rm M}$, hence, validating our assumption, $I_{\rm S} \approx I_{\rm M}$. Furthermore, it is apparent that Pcov is a monotonic decreasing function respect to $\gamma_{\rm D}$ from its definition in (4). On the other hand, the PSE is a unimodal function of $\gamma_{\rm D}$.

The impact of network radius on the performance of both Pcov and PSE is provided in figure 3. As noted in Propositions 6 and 11, both Pcov and PSE are decreasing function of the network radius. Moreover, although Pcov and PSE attain its maximum when $R \to 0$, they are not the same. In fact, Pcov achieves its maximum which is different to one, the PSE, on the contrary, goes to infinity if $R \to 0$ due to the unbounded path-loss model which can be immediately derived from its definition in (5). Looking at the performance of Pcov in Figs. 1 and 3, we experience that they have the same asymptotic value case $\overline{N}$ = 4500, thus, confirming our findings in Remark 10.

Figure 4 studies the performance of both Pcov and PSE versus $\overline{N}$, case $\mathcal{B} < \gamma_{\rm I}\widetilde{\mathcal{C}}$. Again, there is a good agreement between the mathematical framework and the computer-based simulations. As proved in *Proposition* 2, the coverage probability is a convex function with monotonic decreasing property with $\overline{N}$ regardless of the value of $\mathcal{B}$ versus $\gamma_{\rm I}\widetilde{\mathcal{C}}$ and the same

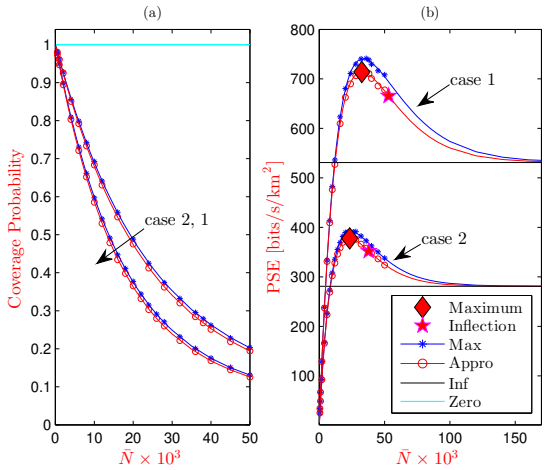


Fig. 4. Coverage probability (a) and potential spectral efficiency (b) versus $\overline{N} = \lambda\pi R^2$, case $\mathcal{B} < \gamma_{\text{I}}\widetilde{\mathcal{C}}$ with two cases: parameters of the first case is provided in Table II and the second case is provided as SF = 8, CR = 0.5, $L_{\text{pac}}$ = 1 byte, $T_{\text{in}}$ = 60 sec, $\gamma_{\text{D}}$ = 6 dBm and $\overline{N}$ = 1500. Solid lines show the exact, the approximation and the asymptotic framework of both Pcov and PSE and are calculated by equations (11), (12), (5) and Propositions 2, 7 respectively. Markers show Monte Carlo simulation. The curves "Inf" correspond to case $\overline{N} \to \infty$ of PSE while the curves "Zero" show Pcov when $\overline{N} \to 0$. The markers "◆" and "★" are the maximum and inflection point from the approximation framework, *Propositions* 7.

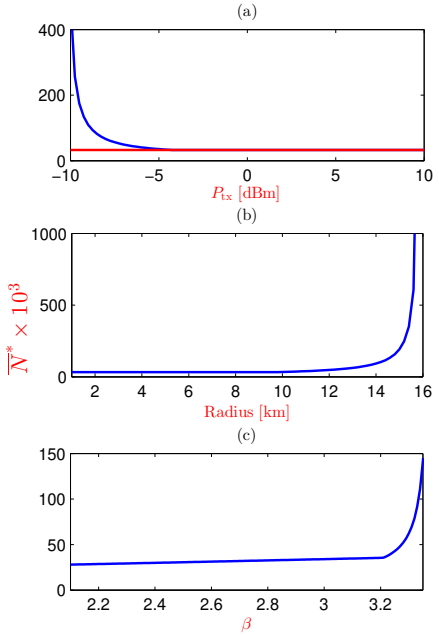


Fig. 5. The trends of $\overline{N}^*$ versus the transmit power (a), $P_{\text{tx}}$; the network radius (b), $R$; and the path-loss exponent, (c), $\beta$. These curves are plotted by using the formula in *Proposition* 7; the red line in case (a) are drawn based on the findings in *Corollary* 1.

observation for case respect to the transmit power and network radius. The PSE, on the other hand, is a unimodal function in this case study. Moreover, we observe that the maximum denoted by "◆", based on the approximated framework provided in *Proposition* 7 is very close to the exact one which can only obtain via the exhaustive search. Furthermore, as the function changes from concavity to convexity, it means that the minimum always appears at the convex region and from the figure, it is evident that the minimum is achieved when $\overline{N} \gg 1$. It, in addition, also means that network densification or increasing $\overline{N}$ does not always boost the PSE. Figure 4 also unveils that there is a contradict behavior of Pcov and PSE respect to the number of end-devices. To be more specific, keep increasing $\overline{N}$ will improve PSE (to some extent), however, the performance of Pcov significantly reduces with this augmentation. Thus, there is a dilemma issue when solving the scalability problem in LoRa networks. From the network perspective, increasing $\overline{N}$ obviously benefits, nonetheless, from the viewpoint of end-devices, increasing $\overline{N}$, of course, soaring the transmission failure. Optimizing the benefits of both sides, however, is out of scope of the current paper and is left for future works. In Fig. 5, we are interested in investigating the behavior of both $\overline{N}^*$ and $\overline{N}^{**}$ for this case study, $\mathcal{B} < \gamma_{\text{I}}\widetilde{\mathcal{C}}$.

To be specific, insights of $\overline{N}^*$ respect to the transmit power, the network radius and the path-loss exponent are shown in Fig. 5(a), 5(b) and 5(c), correspondingly. These figures

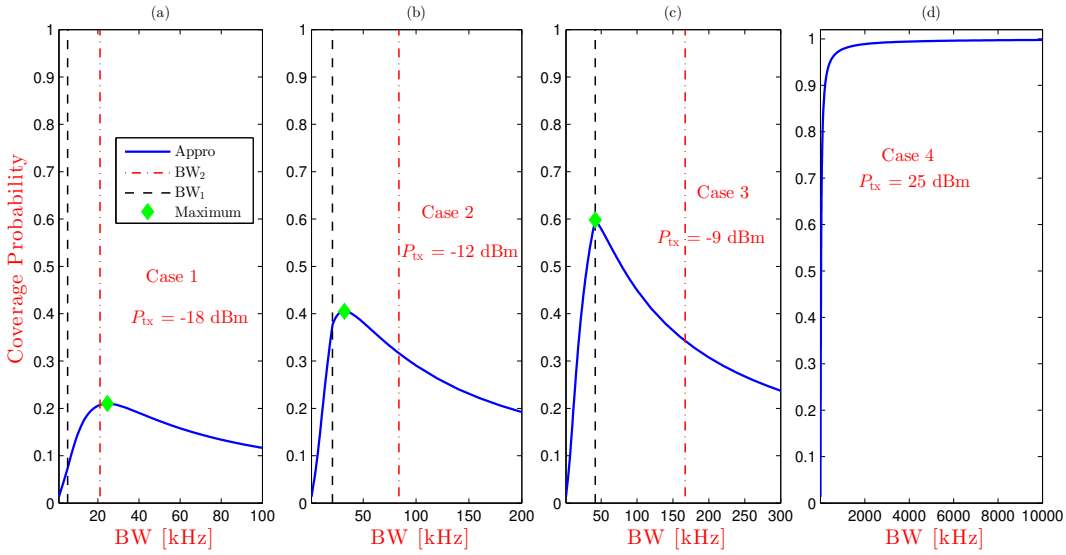


Fig. 6. Coverage probability versus the transmission bandwidth with various scenarios; (a) case 1: $P_{\text{tx}} \leq \frac{\phi_7 \gamma_{\text{D}} \phi_8}{\gamma_{\text{I}} \widetilde{\mathcal{C}} \varsigma_1^*}$; (b) case 2: $P_{\text{tx}} \in \left( \frac{\phi_7 \gamma_{\text{D}} \phi_8}{\gamma_{\text{I}} \widetilde{\mathcal{A}} \varsigma_1^*}, \frac{\phi_7 \gamma_{\text{D}} \phi_8}{\delta \widetilde{\mathcal{C}}} \right]$; (c) case 3: $P_{\text{tx}} > \frac{\phi_7 \gamma_{\text{D}} \phi_8}{\delta \widetilde{\mathcal{C}}}$ and (d) case 4: $P_{\text{tx}} \to \infty$. The marker "◆" is the maximum point which is computed by utilizing the formula in *Proposition* 5. The solid lines are plotted based on the expression (12) and the vertical curves "$\text{BW}_1$" and "$\text{BW}_2$" are obtained according to the condition $\mathcal{B} = \widetilde{\mathcal{C}}$ and $\mathcal{B} = \gamma_{\text{I}} \widetilde{\mathcal{C}}$, respectively.

substantiate our conclusions in *Corollaries* 1, 2 and 3. From the figure, we have following conclusions: i) the smaller the transmit power, the higher the $\overline{N}^*$; ii) the larger the network radius and the path-loss exponent, the bigger the $\overline{N}^*$. Nevertheless, recalling that the necessary condition for this case study is $\mathcal{B} < \gamma_{\text{I}} \widetilde{\mathcal{C}}$. It, consequently, always exists a minimum value of $P_{\text{tx}}$ (maximum for $R$ and $\beta$) so that $\overline{N}^*$ is still a meaningful number, i.e., $0 < \overline{N}^* < \infty$. In fact, $\overline{N}^*$ tends to infinity if $\mathcal{B} \to \gamma_{\text{I}} \widetilde{\mathcal{C}}$. The trends of $\overline{N}^{**}$ respect to the transmit power, the network radius and the path-loss exponent are identical to $\overline{N}^{**}$, thus, we do not report here. Moreover, by checking the trends of Pcov respect to the transmit power, the network radius and the path-loss exponent in Figs. 1(a), 3(a) and 8(a), respectively. It is apparent that decreasing the transmit power (or enhancing the network radius and the path-loss) will primarily decrease the coverage probability. It, again, confirms the dilemma problem between the benefits of end-devices and the whole network's performance.

Fig. 6 confirms our derivations in Proposition 5. In particular, the figure verifies that the coverage probability is a parabola function respect to the transmission bandwidth, BW. Moreover, it also clarifies that depending on the transmit power the maximum point which is denoted by "◆" is located in different non-overlap regions. For example, if $P_{\text{tx}} \leq \frac{\phi_7 \gamma_{\text{D}} \phi_8}{\gamma_{\text{I}} \widetilde{\mathcal{C}} \varsigma_1^*}$, the optimal value is located at the region $\mathcal{B} \geq \gamma_{\text{I}} \widetilde{\mathcal{C}}$ which is the right side of the vertical curve "$\text{BW}_2$" and is computed by using expression, i.e., $\varsigma_{\mathcal{P}}^* = \left[ (\gamma_{\text{I}})^{\delta} \widetilde{\mathcal{A}} \phi_8 (\phi_9)^{-\delta} (\varsigma_1^*)^{-1} \right]^{\frac{1}{1+\delta}}$ in *Proposition* 5 or another case when $P_{\text{tx}} > \frac{\phi_7 \gamma_{\text{D}} \phi_8}{\delta \widetilde{\mathcal{C}}}$ the optimal value is at the crossing point between the vertical curve "$\text{BW}_1$" and the Pcov. Figure 6(d) justifies our findings in *Remark*

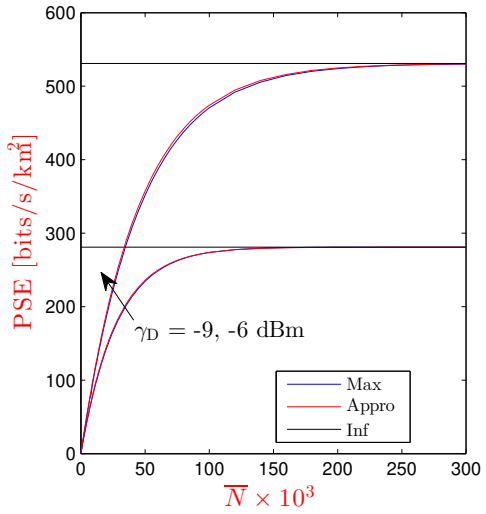


Fig. 7. Potential spectral efficiency of both classes versus $\overline{N}$ case $\mathcal{B} \geq \gamma_I \widetilde{\mathcal{C}}$. The curves are plotted from equations (11), (12), (5), respectively. The curves "Inf" respect to case $\overline{N} \to \infty$ and $P_{tx}$ = - 15 dBm.

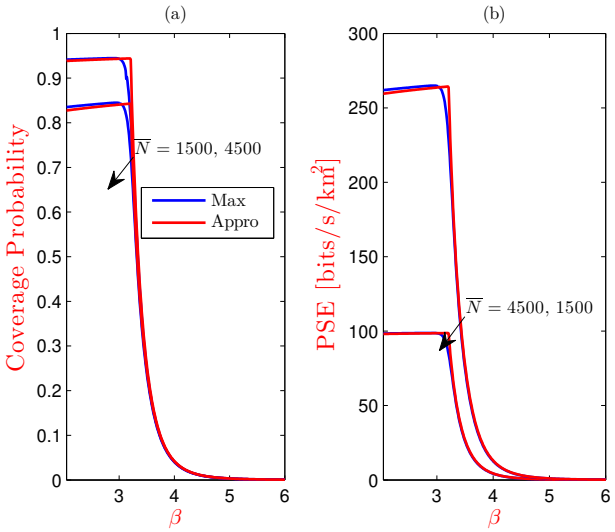


Fig. 8. Coverage probability (a) and potential spectral efficiency (b) versus the path-loss exponent, $\beta$. The curves are plotted based on the expressions (11), (12), (5).

7 that the Pcov simply rises up to one if the transmit power is adequately large or $\varsigma^*_{\mathcal{P}} \to \infty$.

Fig. 7 investigates the insights of PSE when the condition $\mathcal{B} < \gamma_I \widetilde{\mathcal{C}}$, no longer satisfied. Particularly, we see that PSE monotonically increases to its maximum at $\overline{N} \to +\infty$, when $\mathcal{B} \geq \gamma_I \widetilde{\mathcal{C}}$ and justifies our findings in *Proposition* 7. It, however, should be indicated that this case study rarely exists in practical LoRa networks [16] as it requires an extremely small transmit power.

The trends of both Pcov and PSE if changing the path-loss exponent, i.e., $\beta$, are revealed in Fig. 8. This figure illustrates that both Pcov and PSE start increasing moderately when $\beta$ is close to 2 follow by dramatically plunging when $\beta$ is fairly large. Then, they keep decreasing with lower pace.

Figs. 9 and 10 investigate the behaviors of both Pcov and PSE respect to both the transmit power and the average number of end-devices simultaneously. These figures prove the accuracy of our derivations in *Propositions* 4 and 9. In particular, it exists a pair of $\left(\overline{N}, P_{tx}\right)$ that maximizes the PSE. In addition, in Fig. 10, we also observe that keep increasing $\overline{N}$ while fixing $P_{tx}$, the PSE approaches its asymptotic value as reported in Fig. 4. On the other hand, fixing $\overline{N}$ and increasing $P_{tx}$ simply improves the PSE. As for the Pcov, it is a concave function as proven and achieves its maximum when $\overline{N}$ tends to zero accompany with $P_{tx}$ is sufficient large, i.e., $P_{tx} \geq 0$, in Fig. 9.

## VI. Conclusion

In this paper, the comprehensive performance of two vital metrics of LoRa networks, i.e, Pcov and PSE are investigated. Our proposed approximation frameworks are computed in

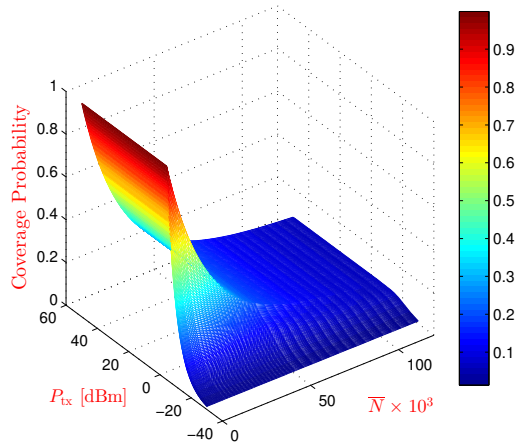


Fig. 9. The coverage probability, $\widetilde{\text{Pcov}}$, as a function of both the average number of EDs, $\overline{N}$ and the transmit power, $P_{\text{tx}}$. The figure is plotted by using (12).

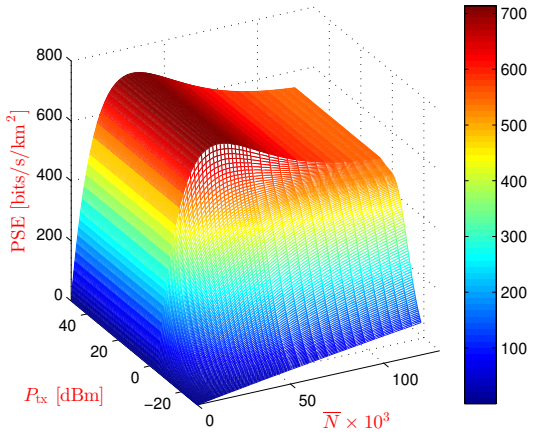


Fig. 10. The potential spectral efficiency, $\widetilde{\text{PSE}}$, respect to both the average number of EDs, $\overline{N}$ and the transmit power, $P_{\text{tx}}$. The figure is plotted by using (5).

closed-form expression and checked by Monte Carlo simulations. Furthermore, the insights of both Pcov and PSE as a function of lots of system parameters, namely, the average number of EDs, the transmit power, the network radius and the bandwidth, are studied based on the proposed mathematical frameworks. Our findings show that there is a counter benefit between the PSE and Pcov respect to the average number of EDs. The transmit power, on the other hand, always bring benefits regardless of the considered metrics, Pcov or PSE.

## APPENDIX I
## PROOF OF EQ. (12)

Let us start re-writing the definition of the approximated coverage probability as follows

$$\begin{aligned}
\widetilde{\text{Pcov}}\left(\gamma_{\text{D}}\right) &\approx \Pr\left\{\widetilde{S}_0/\widetilde{I_{\text{M}}} \geq \gamma_{\text{I}}, P_{\text{tx}}\widetilde{S}_0/\sigma^2 \geq \gamma_{\text{D}}\right\} \\
&= \int_{x=\mathcal{B}}^{\infty} \delta\widetilde{\mathcal{A}} x^{-\delta-1} \exp\left(-\mathcal{G}\mathbf{1}\left(\gamma_{\text{I}}\widetilde{\mathcal{C}} - x\right)\right)\mathbf{1}\left(x - \widetilde{\mathcal{C}}\right)\exp\left(-x^{-\delta}\widetilde{\mathcal{D}}(\gamma_{\text{I}})^{\delta}\mathbf{1}\left(x - \gamma_{\text{I}}\widetilde{\mathcal{C}}\right)\right)dx \\
&\overset{(a)}{=} (\mathcal{G})^{-1}(\gamma_{\text{I}})^{-\delta}\left(1 - \exp\left(-(\gamma_{\text{I}})^{\delta}\widetilde{\mathcal{D}}\left(\max\left\{\mathcal{B}, \gamma_{\text{I}}\widetilde{\mathcal{C}}\right\}\right)^{-\delta}\right)\right) + \widetilde{\mathcal{A}}\exp\left(-\mathcal{G}\right) \\
&\quad \times \left(\left(\max\left\{\widetilde{\mathcal{C}}, \mathcal{B}\right\}\right)^{-\delta} - \left(\gamma_{\text{I}}\widetilde{\mathcal{C}}\right)^{-\delta}\right)\mathbf{1}\left(\gamma_{\text{I}}\widetilde{\mathcal{C}} - \mathcal{B}\right). \qquad (29)
\end{aligned}$$

Here $(a)$ is held by splitting the integration into three cases: i) $\gamma_{\text{I}}\widetilde{\mathcal{C}} \leq \mathcal{B}$; ii) $\widetilde{\mathcal{C}} \leq \mathcal{B} < \gamma_{\text{I}}\widetilde{\mathcal{C}}$ and iii) $\mathcal{B} < \widetilde{\mathcal{C}}$; and utilizing following results: $\int_{x=a}^{b} x^{-c-1}dx = c^{-1}\left(a^{-c} - b^{-c}\right)$ and $\int_{x=a}^{\infty} x^{-c-1}\exp\left(-bx^{-c}\right)dx = (bc)^{-1}\left(1 - \exp\left(-ba^{-c}\right)\right)$, we conclude the proof here.

## APPENDIX II
## PROOF OF PROPOSITION 2

Let us rewrite the Pcov as a function of the average number of EDs as

$$\widetilde{\mathcal{P}}\left(\omega\right)=\phi_1(\mathcal{G}\left(\omega\right))^{-1}\left(1-\exp\left(-\phi_2\mathcal{G}\left(\omega\right)\right)\right)+\phi_3\exp\left(-\mathcal{G}\left(\omega\right)\right)\mathbf{1}\left(\gamma_{\mathrm{I}}\widetilde{\mathcal{C}}-\mathcal{B}\right). \tag{30}$$

In (30), we explicitly represent $\widetilde{\mathrm{Pcov}}\left(\gamma_{\mathrm{D}}\right)$ as a function of $\omega=\overline{N}$ via the term $\mathcal{G}\left(\omega\right)=p_A\omega$; other shorthands, i.e., $\phi_1=\left(\gamma_{\mathrm{I}}\right)^{-\delta}$; $\phi_2=\left(\gamma_{\mathrm{I}}\right)^{\delta}\left(\max\left\{\mathcal{B},\gamma_{\mathrm{I}}\widetilde{\mathcal{C}}\right\}\right)^{-\delta}\widetilde{\mathcal{A}}$ and $\phi_3=\widetilde{\mathcal{A}}\left(\left(\max\left\{\widetilde{\mathcal{C}},\mathcal{B}\right\}\right)^{-\delta}-\left(\gamma_{\mathrm{I}}\widetilde{\mathcal{C}}\right)^{-\delta}\right)$ are independent of $\omega$.

Next, let us take the first-order derivative of (30) respect to $\omega$, we have following

$$\begin{aligned}\dot{\widetilde{\mathcal{P}}}\left(\omega\right)=&-\phi_1\dot{\mathcal{G}}\left(\omega\right)\left(\mathcal{G}\left(\omega\right)\right)^{-2}[1-\exp(-\phi_2\mathcal{G}\left(\omega\right))\left(1+\phi_2\mathcal{G}\left(\omega\right)\right)]\\&-\phi_3\dot{\mathcal{G}}\left(\omega\right)\exp\left(-\mathcal{G}\left(\omega\right)\right)\mathbf{1}\left(\gamma_{\mathrm{I}}\widetilde{\mathcal{C}}-\mathcal{B}\right)\leq 0,\forall\omega\geq 0.\end{aligned} \tag{31}$$

Here $\dot{\widetilde{\mathcal{P}}}\left(\omega\right)$ is always negative because the first-order derivative of $\mathcal{G}\left(\omega\right)$, i.e., $\dot{\mathcal{G}}\left(\omega\right)=p_A\geq 0$ is always positive. As a result, we can state that $\widetilde{\mathrm{Pcov}}\left(\gamma_{\mathrm{D}}\right)$ is monotonically decreasing with $\omega=\overline{N}$.

As for the convexity property, the second-order derivative test is needed, from (31), the second-order derivative of $\widetilde{\mathrm{Pcov}}\left(\gamma_{\mathrm{D}}\right)$ denoted by $\ddot{\widetilde{\mathcal{P}}}\left(\omega\right)$ is provided as follows

$$\begin{aligned}\ddot{\widetilde{\mathcal{P}}}\left(\omega\right)=&\phi_3\left[\dot{\mathcal{G}}\left(\omega\right)\right]^2\exp\left(-\mathcal{G}\left(\omega\right)\right)\mathbf{1}\left(\gamma_{\mathrm{I}}\widetilde{\mathcal{C}}-\mathcal{B}_k\right)\\&+\phi_1\left[\dot{\mathcal{G}}\left(\omega\right)\right]^2\left(\mathcal{G}\left(\omega\right)\right)^{-3}\left(2-\exp\left(-\phi_2\mathcal{G}\left(\omega\right)\right)\left(1+\left(1+\phi_2\mathcal{G}\left(\omega\right)\right)^2\right)\right)\geq 0.\end{aligned} \tag{32}$$

Eq. (32) is always correct as the term $2-\exp\left(-\phi_2\mathcal{G}\left(\omega\right)\right)\left(1+\left(1+\phi_2\mathcal{G}\left(\omega\right)\right)^2\right)$ is a monotonic increasing function respect to $\phi_2\mathcal{G}\left(\omega\right)$ and attains its maximum at $\phi_2\mathcal{G}\left(\omega\right)=0$.

Finally, the asymptotic behavior when $\omega\to+\infty$ can be derived simply from (30) and when $\omega\to 0$ is derived as follows

$$\begin{aligned}\lim_{\omega\to 0}\widetilde{\mathcal{P}}\left(\omega\right)=&\lim_{\omega\to 0}\left(\phi_1\frac{1-\exp\left(-\phi_2\mathcal{G}\left(\omega\right)\right)}{\mathcal{G}\left(\omega\right)}+\phi_3\exp\left(-\mathcal{G}\left(\omega\right)\right)\mathbf{1}\left(\gamma_{\mathrm{I}}\widetilde{\mathcal{C}}-\mathcal{B}\right)\right)\\\overset{(a)}{=}&\phi_1\phi_2+\phi_3\mathbf{1}\left(\gamma_{\mathrm{I}}\widetilde{\mathcal{C}}-\mathcal{B}\right),\end{aligned} \tag{33}$$

where $(a)$ is obtained by using L'Hôpital's rule and we close the proof here.

## APPENDIX III
## PROOF OF PROPOSITION 3

At first, let us rewrite the approximation framework of Pcov as a function of the transmit power, i.e., $\xi = P_{\text{tx}}$, as follows:

$$\begin{aligned}\widetilde{\mathcal{P}}\left(\xi\right) =& \phi_4\left(1-\exp\left(-\phi_5\Big(\max\left\{\mathcal{B}\left(\xi\right),\gamma_{\text{I}}\widetilde{\mathcal{C}}\right\}\Big)^{-\delta}\right)\right)\\ &+\phi_6\left(\Big(\max\left\{\mathcal{B}\left(\xi\right),\widetilde{\mathcal{C}}\right\}\Big)^{-\delta}-\left(\gamma_{\text{I}}\widetilde{\mathcal{C}}\right)^{-\delta}\right)\mathbf{1}\left(\gamma_{\text{I}}\widetilde{\mathcal{C}}-\mathcal{B}\left(\xi\right)\right),\end{aligned} \tag{34}$$

where $\phi_4 = (\mathcal{G})^{-1}(\gamma_{\text{I}})^{-\delta}; \phi_5 = (\gamma_{\text{I}})^{\delta}\widetilde{\mathcal{A}}\mathcal{G}; \phi_6 = \widetilde{\mathcal{A}}\exp\left(-\mathcal{G}\right)$ are shorthand and independent of $\xi$. In (34), it is noted that Pcov depends on $\xi$ through the unique term $\mathcal{B}\left(\xi\right) = \sigma^2\gamma_{\text{D}}\xi^{-1}$. Next, taking the first-order derivative of (34) respect to $\xi$, we have

$$\begin{aligned}\dot{\widetilde{\mathcal{P}}}\left(\xi\right) =& -\delta\widetilde{\mathcal{A}}\dot{\mathcal{B}}\left(\xi\right)\left(\mathcal{B}(\xi)\right)^{-\delta-1}\Big[\exp\left(-(\gamma_{\text{I}})^{\delta}\widetilde{\mathcal{A}}\mathcal{G}(\mathcal{B}\left(\xi\right))^{-\delta}\right)\\ &\times\mathbf{1}\left(\mathcal{B}\left(\xi\right)-\gamma_{\text{I}}\widetilde{\mathcal{C}}\right)+\exp\left(-\mathcal{G}\right)\mathbf{1}\left(\gamma_{\text{I}}\widetilde{\mathcal{C}}-\mathcal{B}\left(\xi\right)\right)\mathbf{1}\left(\mathcal{B}\left(\xi\right)-\widetilde{\mathcal{C}}\right)\Big]\geq 0,\forall\xi\geq 0,\end{aligned} \tag{35}$$

where $\dot{\mathcal{B}}\left(\xi\right) = -\sigma^2\gamma_{\text{D}}\xi^{-2} \leq 0$. The second-order property of the Pcov is derived as follows

$$\begin{aligned}\ddot{\widetilde{\mathcal{P}}}\left(\xi\right) =& -\delta\phi_4\phi_5\exp\left(-\phi_5(\mathcal{B}\left(\xi\right))^{-\delta}\right)\left((\mathcal{B}\left(\xi\right))^{-\delta-2}\mathcal{T}_0\left(\xi\right)+\phi_5\delta\Big[\dot{\mathcal{B}}\left(\xi\right)(\mathcal{B}\left(\xi\right))^{-\delta-1}\Big]^2\right)\\ &\times\mathbf{1}\left(\mathcal{B}\left(\xi\right)-\gamma_{\text{I}}\widetilde{\mathcal{C}}\right)-\delta\phi_6(\mathcal{B}\left(\xi\right))^{-\delta-2}\mathcal{T}_0\left(\xi\right)\mathbf{1}\left(\gamma_{\text{I}}\widetilde{\mathcal{C}}-\mathcal{B}\left(\xi\right)\right)\mathbf{1}\left(\mathcal{B}\left(\xi\right)-\widetilde{\mathcal{C}}\right)\leq 0.\end{aligned} \tag{36}$$

Here $\mathcal{T}_0\left(\xi\right) = \ddot{\mathcal{B}}\left(\xi\right)\mathcal{B}\left(\xi\right)-(\delta+1)\left(\dot{\mathcal{B}}\left(\xi\right)\right)^2 = \left(\sigma^2\gamma_{\text{D}}\xi^{-2}\right)^2\left[2-(\delta+1)\right]\geq 0, \delta<1$. From (36), we are able to state that the coverage probability is a concave function respect to the transmit power. Finally, the asymptotic of $\widetilde{\mathcal{P}}\left(\xi\right)$ when $\xi\to 0$ and $\xi\to+\infty$ are directly drawn from (34) by substituting $\mathcal{B}\left(\xi\to 0\right) = +\infty$ and $\mathcal{B}\left(\xi\to+\infty\right) = 0$, respectively; and we finish the proof here.

## APPENDIX IV
## PROOF OF PROPOSITION 5

In this section, the behavior of Pcov as a function of BW is investigated. Let us start rewriting the Pcov as a function of BW as follows

$$\begin{aligned}&\widetilde{\mathcal{P}}\left(\varsigma=\text{BW}\right) = \left(\mathcal{G}\left(\varsigma\right)\right)^{-1}(\gamma_{\text{I}})^{-\delta}\left(1-\exp\left(-(\gamma_{\text{I}})^{\delta}\widetilde{\mathcal{A}}\mathcal{G}\left(\varsigma\right)\left(\max\left\{\mathcal{B}\left(\varsigma\right),\gamma_{\text{I}}\widetilde{\mathcal{C}}\right\}\right)^{-\delta}\right)\right)\\ &+\widetilde{\mathcal{A}}\exp\left(-\mathcal{G}\left(\varsigma\right)\right)\left(\Big(\max\left\{\widetilde{\mathcal{C}},\mathcal{B}\left(\varsigma\right)\right\}\Big)^{-\delta}-\left(\gamma_{\text{I}}\widetilde{\mathcal{C}}\right)^{-\delta}\right)\mathbf{1}\left(\gamma_{\text{I}}\widetilde{\mathcal{C}}-\mathcal{B}\left(\varsigma\right)\right)\\ &=\mathcal{V}_1\left(\varsigma\right)\mathbf{1}\left(\mathcal{B}\left(\varsigma\right)-\gamma_{\text{I}}\widetilde{\mathcal{C}}\right)+\mathcal{V}_3\left(\varsigma\right)\mathbf{1}\left(\widetilde{\mathcal{C}}-\mathcal{B}\left(\varsigma\right)\right)+\mathcal{V}_2\left(\varsigma\right)\mathbf{1}\left(\gamma_{\text{I}}\widetilde{\mathcal{C}}-\mathcal{B}\left(\varsigma\right)\right)\mathbf{1}\left(\mathcal{B}\left(\varsigma\right)-\widetilde{\mathcal{C}}\right),\end{aligned} \tag{37}$$

where $\mathcal{B}\left(\varsigma\right) = \phi_9\varsigma \Rightarrow \dot{\mathcal{B}}\left(\varsigma\right) = \phi_9 \geq 0$; $\mathcal{G}\left(\varsigma\right) = \frac{\phi_8}{\varsigma} \Rightarrow \dot{\mathcal{G}}\left(\varsigma\right) = -\frac{\phi_8}{\varsigma^2} \leq 0$; $\phi_8$, $\phi_9$ are defined in Proposition 5.

From the first sight, (37) is too complicated to figure out the behavior of Pcov as a function of BW. Hence, we split the Pcov into three cases denoted by $\mathcal{V}_s\left(\varsigma\right)$, $s \in \{1,2,3\}$. We are going to inspect the behavior for each case; let us begin with $\mathcal{V}_1\left(\varsigma\right)$ as

$$\begin{aligned}\mathcal{V}_1\left(\varsigma\right) =& \frac{\left(\gamma_{\text{I}}\right)^{-\delta}}{\mathcal{G}\left(\varsigma\right)}\left(1-\exp\left(-\left(\gamma_{\text{I}}\right)^{\delta}\widetilde{\mathcal{A}}\mathcal{G}\left(\varsigma\right)\left(\mathcal{B}(\varsigma)\right)^{-\delta}\right)\right)\\ \dot{\mathcal{V}}_1\left(\varsigma\right) =& \frac{d\mathcal{V}_1\left(\varsigma\right)}{d\varsigma} = \frac{\left(\gamma_{\text{I}}\right)^{-\delta}}{\phi_8}\mathcal{T}_1\left(\left(\gamma_{\text{I}}\right)^{\delta}\widetilde{\mathcal{A}}\mathcal{G}\left(\varsigma\right)\left(\mathcal{B}(\varsigma)\right)^{-\delta}\right)\end{aligned} \tag{38}$$

Here $\mathcal{T}_1\left(t\right) = 1-\exp\left(-t\right)\left(t\left(1+\delta\right)+1\right),\ t \geq 0$. It is straightforward to claim that $\mathcal{T}_1$ changes from negative to positive and cross the horizontal axis at $t^* \geq \delta \geq 0$ or $\mathcal{T}_1\left(t^*\right)=0$. So $\dot{\mathcal{V}}_1\left(\varsigma\right)$ is changing from positive to negative as $\left(\gamma_{\text{I}}\right)^{\delta}\widetilde{\mathcal{A}}\mathcal{G}\left(\varsigma\right)\left(\mathcal{B}(\varsigma)\right)^{-\delta}$ is a decreasing function of $\varsigma$. As a result, $\mathcal{V}_1\left(\varsigma\right)$ is a unimodal function and attains its maximum at $\varsigma^*_{\mathcal{P}}$ given as follows

$$\varsigma_1^* = \left(\gamma_{\text{I}}\right)^{\delta}\widetilde{\mathcal{A}}\phi_8(\phi_9)^{-\delta}(\varsigma^*_{\mathcal{P}})^{-\delta-1} \Rightarrow \varsigma^*_{\mathcal{P}} = \left[\left(\gamma_{\text{I}}\right)^{\delta}\widetilde{\mathcal{A}}\phi_8(\phi_9)^{-\delta}(\varsigma_1^*)^{-1}\right]^{\frac{1}{\delta+1}}, \tag{39}$$

where $\varsigma_1^*$ is the solution of $\mathcal{T}_1\left(\varsigma_1^*\right)=0$. Recalling that the necessary condition for this case study is: $\mathcal{B}\left(\varsigma\right) \geq \gamma_{\text{I}}\widetilde{\mathcal{C}} \Leftrightarrow \varsigma \geq \frac{\gamma_{\text{I}}\widetilde{\mathcal{C}}}{\phi_9}$, so the sufficient condition that the optimal value of $\varsigma$, i.e., $\varsigma^*$, belongs to this region is following

$$\varsigma^*_{\mathcal{P}} \geq \varsigma \Leftrightarrow \left[\left(\gamma_{\text{I}}\right)^{\delta}\widetilde{\mathcal{A}}\phi_8(\phi_9)^{-\delta}(\varsigma_1^*)^{-1}\right]^{\frac{1}{\delta+1}} \geq \frac{\gamma_{\text{I}}\widetilde{\mathcal{C}}}{\phi_9} \Leftrightarrow P_{\text{tx}} \leq \frac{\phi_7\gamma_{\text{D}}\phi_8}{\gamma_{\text{I}}\widetilde{\mathcal{C}}\varsigma_1^*} \tag{40}$$

In short, for this case study, Pcov is a unimodal function and reaches its maximum at $\varsigma^*_{\mathcal{P}}$ provided that $P_{\text{tx}} \leq \frac{\phi_7\gamma_{\text{D}}\phi_8}{\gamma_{\text{I}}\widetilde{\mathcal{C}}\varsigma_1^*}$, otherwise, Pcov monotonically decreases with $\varsigma$ since $\varsigma$ is greater than the maximal value as $\varsigma^*_{\mathcal{P}} \leq \frac{\gamma_{\text{I}}\widetilde{\mathcal{C}}}{\phi_9} \leq \varsigma$. Now, let us go to the second case

$$\begin{aligned}\mathcal{V}_2\left(\varsigma\right) =& \frac{\left(\gamma_{\text{I}}\right)^{-\delta}}{\mathcal{G}\left(\varsigma\right)}\left(1-\exp\left(-\mathcal{G}\left(\varsigma\right)\right)\right)+\widetilde{\mathcal{A}}\exp\left(-\mathcal{G}\left(\varsigma\right)\right)\left(\left(\mathcal{B}\left(\varsigma\right)\right)^{-\delta}-\left(\gamma_{\text{I}}\widetilde{\mathcal{C}}\right)^{-\delta}\right)\\ \dot{\mathcal{V}}_2\left(\varsigma\right) =& \varsigma^{-1}\widetilde{\mathcal{A}}\left(\mathcal{B}\left(\varsigma\right)\right)^{-\delta}\exp\left(-\mathcal{G}\left(\varsigma\right)\right)\left(\mathcal{G}\left(\varsigma\right)-\delta\right)+\left(\gamma_{\text{I}}\right)^{-\delta}\left(\varsigma\mathcal{G}\left(\varsigma\right)\right)^{-1}\\ &\times\left(1-\exp\left(-\mathcal{G}\left(\varsigma\right)\right)\left(1+\mathcal{G}\left(\varsigma\right)+\left(\mathcal{G}\left(\varsigma\right)\right)^2\right)\right).\end{aligned} \tag{41}$$

By using the property $\left(\gamma_{\text{I}}\right)^{-\delta} = \widetilde{\mathcal{A}}\left(\gamma_{\text{I}}\widetilde{\mathcal{C}}\right)^{-\delta} \leq \widetilde{\mathcal{A}}(\mathcal{B}\left(\varsigma\right))^{-\delta} \leq \widetilde{\mathcal{A}}\left(\widetilde{\mathcal{C}}\right)^{-\delta} = 1$ and assuming that $\mathcal{G}\left(\varsigma\right) \leq \delta$, (41) can be written as follows

$$\dot{\mathcal{V}}_2\left(\varsigma\right) \leq \left(\gamma_{\text{I}}\right)^{-\delta}\left(\varsigma\mathcal{G}\left(\varsigma\right)\right)^{-1}\mathcal{T}_1\left(\mathcal{G}\left(\varsigma\right)\right) \leq 0. \tag{42}$$

Eq. (42) is obtained by the fact that $\mathcal{T}_1\left(t\right) \leq 0$ providing that $t = \mathcal{G}\left(\varsigma\right) \leq \delta \leq t^*$ as proven in previous case. The sufficient condition for this scenario is $\frac{\phi_{14}}{\delta} \leq \frac{P_{\text{tx}}\widetilde{\mathcal{C}}}{\phi_7\gamma_{\text{D}}} \Leftrightarrow P_{\text{tx}} \geq \frac{\phi_7\gamma_{\text{D}}\phi_8}{\delta\widetilde{\mathcal{C}}}$. This condition is obtained by combining two following conditions, $\mathcal{G}\left(\varsigma\right) \leq \delta \Leftrightarrow \frac{\phi_8}{\delta} \leq \varsigma$ and

$\widetilde{\mathcal{C}} \leq \mathcal{B}(\varsigma) \Leftrightarrow \frac{P_{\text{tx}}\widetilde{\mathcal{C}}}{\phi_7\gamma_{\text{D}}} \leq \varsigma$. Now, considering another scenario, $\mathcal{G}(\varsigma) \geq \delta$, then we have

$$\dot{\mathcal{V}}_2(\varsigma) \geq (\gamma_{\text{I}})^{-\delta} (\varsigma\mathcal{G}(\varsigma))^{-1} \mathcal{T}_1(\mathcal{G}(\varsigma)). \tag{43}$$

From previous case, $\dot{\mathcal{V}}_1(\varsigma)$, we know that $\mathcal{T}_1(\mathcal{G}(\varsigma))$ changes from negative to positive respect to $\mathcal{G}(\varsigma)$, thus, the right hand side of (43) also changes from negative to positive with $\mathcal{G}(\varsigma)$ or from positive to negative respect to $\varsigma$. As a result, the sufficient condition that $\dot{\mathcal{V}}_2(\varsigma)$ is positive is $\mathcal{G}(\varsigma) \geq \varsigma_1^* \geq \delta$ and $\mathcal{B}(\varsigma) < \gamma_{\text{I}}\widetilde{\mathcal{C}}$, then, we have $P_{\text{tx}} < \frac{\phi_7\gamma_{\text{D}}\phi_8}{\gamma_{\text{I}}\widetilde{\mathcal{C}}\varsigma_1^*}$. Finally, Pcov is a unimodal function with $\varsigma$ and attains its maximum at $\varsigma_2^*$ that is the solution of (41) if $\delta \leq \mathcal{G}(\varsigma) \leq \varsigma_1^*$ and the corresponding condition is $P_{\text{tx}} \in \left(\frac{\phi_7\gamma_{\text{D}}\phi_8}{\gamma_{\text{I}}\widetilde{\mathcal{C}}\varsigma_1^*}, \frac{\phi_7\gamma_{\text{D}}\phi_8}{\delta\widetilde{\mathcal{C}}}\right]$. Now, let us move to the last case as follows

$$\begin{aligned}
\mathcal{V}_3(\varsigma) =& \frac{(\gamma_{\text{I}})^{-\delta}}{\mathcal{G}(\varsigma)} (1 - \exp(-\mathcal{G}(\varsigma))) + \exp(-\mathcal{G}(\varsigma)) \left(1 - (\gamma_{\text{I}})^{-\delta}\right) \\
\dot{\mathcal{V}}_3(\varsigma) =& -\frac{(\gamma_{\text{I}})^{-\delta}\dot{\mathcal{G}}(\varsigma)}{(\mathcal{G}(\varsigma))^2} \underbrace{(1 - \exp(-\mathcal{G}(\varsigma))(1 + \mathcal{G}(\varsigma)))}_{\geq 0} \\
& - \dot{\mathcal{G}}(\varsigma) \exp(-\mathcal{G}(\varsigma)) \left(1 - (\gamma_{\text{I}})^{-\delta}\right) \geq 0, \forall \varsigma \geq 0.
\end{aligned} \tag{44}$$

From (44), it is apparent that Pcov in this case is increasing with $\varsigma$ and approaches its maximum at $\mathcal{B}(\varsigma) = \widetilde{\mathcal{C}} \Leftrightarrow \varsigma_{\mathcal{P}}^* = \frac{P_{\text{tx}}\widetilde{\mathcal{C}}}{\phi_9\gamma_{\text{D}}}$.

Finally, by combining the results from three above cases, we conclude that Pcov is a unimodal function of $\varsigma$ and its optimal value, $\varsigma_{\mathcal{P}}^*$, is computed in (17) and we conclude the proof here.

## APPENDIX V
## PROOF OF PROPOSITION 7

Let us first re-write the $\widetilde{\text{PSE}}$ as a function of $\omega$ as follows

$$\widetilde{\text{PSE}} = \widetilde{\mathcal{S}}(\omega) = \lambda^{\mathcal{A}}\text{BW}\log_2(1 + \gamma_{\text{D}})\widetilde{\text{Pcov}}(\gamma_{\text{D}}) = \phi_{10}\mathcal{G}(\omega)\widetilde{\mathcal{P}}(\omega) \tag{45}$$

where $\mathcal{G}(\omega) = p_A\omega$, $\phi_{10} = \frac{\text{BW}\log_2(1+\gamma_{\text{D}})}{\pi R^2}$. Taking the first-order derivative respect to $\omega$, we have

$$\begin{aligned}
\dot{\widetilde{\mathcal{S}}}(\omega) =& d\widetilde{\mathcal{S}}(\omega)/d\omega = \phi_{10}\left[\dot{\mathcal{G}}(\omega)\widetilde{\mathcal{P}}(\omega) + \mathcal{G}(\omega)\dot{\widetilde{\mathcal{P}}}(\omega)\right] \\
=& \phi_1\phi_2\dot{\mathcal{G}}(\omega)\exp(-\phi_2\mathcal{G}(\omega)) + \phi_3\dot{\mathcal{G}}(\omega)(1 - \mathcal{G}(\omega))\exp(-\mathcal{G}(\omega))\mathbf{1}\left(\gamma_{\text{I}}\widetilde{\mathcal{C}} - \mathcal{B}\right)
\end{aligned} \tag{46}$$

In (46), we ignore the constant term $\phi_{10}$. From (46), we directly hold following conclusion: $\dot{\mathcal{S}}(\omega) \geq 0$ if $\mathcal{B} \geq \gamma_{\text{I}}\widetilde{\mathcal{C}}$. As for case $\mathcal{B} < \gamma_{\text{I}}\widetilde{\mathcal{C}}$, we have $\phi_2 = 1$, so (46) can be rewritten as follows

$$\dot{\mathcal{S}}(\omega) = (\phi_1 + \phi_3 - \phi_3\mathcal{G}(\omega))\dot{\mathcal{G}}(\omega)\exp(-\mathcal{G}(\omega)). \tag{47}$$

From (47), it is quite trivial to conduct following conclusion: $\widetilde{\mathcal{S}}(\omega)$ attains its maximum at $\omega^* = (p_A)^{-1}(1+\phi_1/\phi_3)$. To study the asymptotic behavior of $\widetilde{\mathcal{S}}(\omega)$ when $\omega$ goes to either zero or infinity, we re-write the PSE as follows

$$\widetilde{\mathcal{S}}(\omega) = \phi_{10}\phi_1\left(1-\exp\left(-\phi_2\mathcal{G}(\omega)\right)\right) + \phi_{10}\phi_3\mathcal{G}(\omega)\exp\left(-\mathcal{G}(\omega)\right)\mathbf{1}\left(\gamma_{\mathrm{I}}\widetilde{\mathcal{C}} - \mathcal{B}\right). \tag{48}$$

From (48), it is facile to conclude that $\omega \to 0 \Rightarrow \widetilde{\mathcal{S}}(\omega) \to 0$. As for case $\omega \to \infty$, we have following

$$\lim_{\omega\to\infty}\left(\widetilde{\mathcal{S}}(\omega)\right) \overset{(a)}{=} \phi_1\phi_{10} = (\gamma_{\mathrm{I}})^{-\delta}\frac{\mathrm{BW}\log_2(1+\gamma_{\mathrm{D}})}{\pi R^2} \tag{49}$$

where $(a)$ is held by using L'Hôpital's rule. Now, let us go to study the convexity property of the PSE, we have

$$\begin{aligned}\ddot{\widetilde{\mathcal{S}}}(\omega) =& -2\phi_1\dot{\mathcal{G}}(\omega)\left(\mathcal{G}(\omega)\right)^{-2}\left[1-\exp\left(-\phi_2\mathcal{G}(\omega)\right)\left(1+\phi_2\mathcal{G}(\omega)\right)\right] \\ &+\left[-2\phi_3\dot{\mathcal{G}}(\omega)\exp\left(-\mathcal{G}(\omega)\right)+\phi_3\dot{\mathcal{G}}(\omega)\mathcal{G}(\omega)\exp\left(-\mathcal{G}(\omega)\right)\right] \\ &\times\mathbf{1}\left(\gamma_I\widetilde{\mathcal{C}}-\mathcal{B}\right)+\phi_1\dot{\mathcal{G}}(\omega)(\mathcal{G}(\omega))^{-2}\left(2-\exp\left(-\phi_2\mathcal{G}(\omega)\right)\left(1+\left(1+\phi_2\mathcal{G}(\omega)\right)^2\right)\right)\end{aligned} \tag{50}$$

Here, we ignore the constant term $\phi_{10}p_A$. Now, considering the first case where $\mathcal{B} \geq \gamma_{\mathrm{I}}\widetilde{\mathcal{C}}$ and after some manipulations, (50) can be written as

$$\ddot{\widetilde{\mathcal{S}}}(\omega) = -\phi_1\dot{\mathcal{G}}(\omega)\left(\phi_2\right)^2\exp\left(-\phi_2\mathcal{G}(\omega)\right) \leq 0 \tag{51}$$

As a consequence, PSE is a concave function for this case study and let us consider the remain case $\mathcal{B} < \gamma_{\mathrm{I}}\widetilde{\mathcal{C}}$, (50) is written as

$$\ddot{\widetilde{\mathcal{S}}}(\omega) = -\dot{\mathcal{G}}(\omega)\exp\left(-\mathcal{G}(\omega)\right)\left(\phi_1+\phi_3\left(2-\mathcal{G}(\omega)\right)\right) \tag{52}$$

In (52), it is straightforward to identify the inflection point at $\omega^{**} = (p_A)^{-1}\left(2+\frac{\phi_1}{\phi_3}\right)$ where the PSE changes from concave to convex respect to $\omega$. Finally, from (46), (47), (51) and (52), we summarize that the PSE is monotonic increasing with concavity property providing that $\mathcal{B} \geq \gamma_{\mathrm{I}}\widetilde{\mathcal{C}}$; otherwise, it is a unimodal function and changing from concave to convex, we conclude the proof here.

## APPENDIX VI
## PROOF OF PROPOSITION 9

In this section, the same approach as Proposition 4 is utilized, let us formulate the Hessian matrix and its determinant as follows

$$H_{\widetilde{\mathcal{S}}}(\omega,\xi)=\begin{bmatrix}\frac{\partial^2\widetilde{\mathcal{S}}(\omega,\xi)}{\partial^2\omega} & \frac{\partial^2\widetilde{\mathcal{S}}(\omega,\xi)}{\partial\omega\partial\xi}\\ \frac{\partial^2\widetilde{\mathcal{S}}(\omega,\xi)}{\partial\xi\partial\omega} & \frac{\partial^2\widetilde{\mathcal{S}}(\omega,\xi)}{\partial^2\xi}\end{bmatrix}$$

$$\text{Det}\left\{H_{\widetilde{\mathcal{S}}}(\omega,\xi)\right\}=\frac{\partial^2\widetilde{\mathcal{S}}(\omega,\xi)}{\partial^2\omega}\frac{\partial^2\widetilde{\mathcal{S}}(\omega,\xi)}{\partial^2\xi}-\left(\frac{\partial^2\widetilde{\mathcal{S}}(\omega,\xi)}{\partial\omega\partial\xi}\right)^2 \tag{53}$$

From Propositions 7 and 8, we have $\frac{\partial^2\widetilde{\mathcal{S}}(\omega,\xi)}{\partial^2\omega}=-p_A\phi_{10}\phi_1\mathcal{G}(\omega)(\phi_2)^2\exp(-\phi_2\mathcal{G}(\omega))\leq 0$ when $\gamma_{\text{I}}\widetilde{\mathcal{C}}\leq\mathcal{B}$; $\frac{\partial^2\widetilde{\mathcal{S}}(\omega,\xi)}{\partial^2\omega}=-p_A\phi_{10}\dot{\mathcal{G}}(\omega)\exp(-\mathcal{G}(\omega))(\phi_1+\phi_3(2-\mathcal{G}(\omega)))$ when $\gamma_{\text{I}}\widetilde{\mathcal{C}}>\mathcal{B}$; $\frac{\partial^2\widetilde{\mathcal{S}}(\omega,\xi)}{\partial^2\xi}\leq 0$ when $\widetilde{\mathcal{C}}\leq\mathcal{B}$ and $\frac{\partial^2\widetilde{\mathcal{S}}(\omega,\xi)}{\partial^2\xi}=0$ when $\widetilde{\mathcal{C}}>\mathcal{B}$.

It should be noted that different to the coverage probability, the PSE, from the first sight, is impossible to identify that PSE is either concave or convex respect to both $\omega$ and $\xi$. The mixed partial derivative of $\omega$ and $\xi$, as a result, is required and is given as

$$\begin{aligned}\frac{\partial^2\widetilde{\mathcal{S}}(\omega,\xi)}{\partial\omega\partial\xi}=&\delta\dot{\mathcal{B}}(\xi)(\mathcal{B}(\xi))^{-\delta-1}\widetilde{\mathcal{A}}\dot{\mathcal{G}}(\omega)\exp\left(-(\gamma_{\text{I}})^{\delta}(\mathcal{B}(\xi))^{-\delta}\widetilde{\mathcal{A}}\mathcal{G}(\omega)\right)\mathbf{1}\left(\mathcal{B}(\xi)-\gamma_{\text{I}}\widetilde{\mathcal{C}}\right)\\&\times\left((\gamma_{\text{I}})^{\delta}(\mathcal{B}(\xi))^{-\delta}\widetilde{\mathcal{A}}\mathcal{G}(\omega)-1\right)-\mathbf{1}\left(\gamma_{\text{I}}\widetilde{\mathcal{C}}-\mathcal{B}(\xi)\right)\mathbf{1}\left(\mathcal{B}(\xi)-\widetilde{\mathcal{C}}\right)\\&\times\delta(\mathcal{B}(\xi))^{-\delta-1}\dot{\mathcal{B}}(\xi)\dot{\mathcal{G}}(\omega)\widetilde{\mathcal{A}}(1-\mathcal{G}(\omega))\exp(-\mathcal{G}(\omega))\geq 0\end{aligned} \tag{54}$$

Having all the necessary derivative, we are going to check the sign of the determinant of Hessian. Let us firstly consider case $\mathcal{B}(\xi)\geq\gamma_{\text{I}}\widetilde{\mathcal{C}}$ as

$$\begin{aligned}\text{Det}\{H_{\widetilde{\mathcal{S}}}(\omega,\xi)\}=&\delta\left(\phi_{10}\widetilde{\mathcal{A}}\dot{\mathcal{G}}(\omega)\dot{\mathcal{B}}(\xi)(\mathcal{B}(\xi))^{-\delta-1}\exp\left(-\widetilde{\mathcal{A}}\mathcal{G}(\omega)(\gamma_{\text{I}})^{\delta}(\mathcal{B}(\xi))^{-\delta}\right)\right)^2\\&\times\left[\left(\mathcal{G}(\omega)(\gamma_{\text{I}})^{\delta}(\mathcal{B}(\xi))^{-\delta}\widetilde{\mathcal{A}}\right)(1+\delta)-\delta\right]\end{aligned} \tag{55}$$

From (55), it is obvious that the sign of the determinant merely relies on the term inside the bracket and denoted by $\mathcal{T}_2(\omega,\xi)=\left(\mathcal{G}(\omega)(\gamma_{\text{I}})^{\delta}(\mathcal{B}(\xi))^{-\delta}\widetilde{\mathcal{A}}\right)(1+\delta)-\delta$. In addition, $\mathcal{T}_2(\omega,\xi)$ can be either positive or negative as well which depends on the pair of $(\omega,\xi)$. It, as a consequence, always exists pair of $(\omega,\xi)$ which act as an inflection point of PSE providing that $\mathcal{B}(\xi)\geq\gamma_{\text{I}}\widetilde{\mathcal{C}}$.

Now, let us move to the second case study where following condition is satisfied $\widetilde{\mathcal{C}}\leq\mathcal{B}(\xi)<\gamma_{\text{I}}\widetilde{\mathcal{C}}$. The determinant of this case study is provided as

$$\begin{aligned}\text{Det}\left\{H_{\widetilde{\mathcal{S}}}(\omega,\xi)\right\}=&\delta\widetilde{\mathcal{A}}(\mathcal{B}(\xi))^{-\delta-2}\left(\phi_{10}\exp(-\mathcal{G}(\omega))\dot{\mathcal{G}}(\omega)\dot{\mathcal{B}}(\xi)\right)^2\\&\times\left(\widetilde{\mathcal{A}}(\mathcal{B}(\xi))^{-\delta}\left((1-\delta)-(1-\mathcal{G}(\omega))^2\right)-\mathcal{G}(\omega)(1-\delta)(\gamma_{\text{I}})^{-\delta}(1-\mathcal{G}(\omega))^2\right)\end{aligned} \tag{56}$$

It is reminded that from Proposition 7, we have $\frac{\partial^2 \widetilde{\mathcal{S}}(\omega,\xi)}{\partial^2 \omega} \geq 0$ providing that $\mathcal{G}(\omega) \geq (2+\phi_1/\phi_3)$ so $\text{Det}\left\{H_{\widetilde{\mathcal{S}}}(\omega,\xi)\right\} \leq 0$. However, looking at (56), it is obvious that it can be either positive or negative, e.g., if $(1-\delta)-(1-\mathcal{G}(\omega))^2 \leq 0 \Leftrightarrow \mathcal{G}(\omega) < 1-\sqrt{1-\delta} \cup \mathcal{G}(\omega) > 1+\sqrt{1-\delta}$ then (56) is negative; on the other hand, if $\mathcal{G}(\omega)=1$, (56) is positive regardless of the value of $\mathcal{B}(\xi)$. Consequently, it always exists pair of $(\omega,\xi)$ which act as an inflection point of PSE providing that $\widetilde{\mathcal{C}} \leq \mathcal{B}(\xi) < \gamma_{\text{I}}\widetilde{\mathcal{C}}$.

Now, let us consider the last case study where $\mathcal{B}(\xi) < \widetilde{\mathcal{C}}$, the determinant of this case study is equal to zero since both second-order partial derivative respect to $\xi$, i.e., $\frac{\partial^2 \widetilde{\mathcal{S}}(\omega,\xi)}{\partial^2 \xi}$ and the mixed derivative, $\frac{\partial^2 \widetilde{\mathcal{S}}(\omega,\xi)}{\partial \omega \partial \xi}$, are equal to zero.

Finally, by combining these above findings, the PSE as a function of both density of EDs and the transmit power is either a concave or convex function and always exists pair of $(\omega,\xi)$ that the PSE changes it properties.

## REFERENCES


[1] L.-T. Tu, A. Bradai and Y. Pousset, "A New Closed-Form Expression of the Coverage Probability for Different QoS in LoRa Networks", in Proc. ICC, 2020, accepted for publication.

[2] E. Rogers, "Encouraging intelligent efficiency study of policy opportunities," *Energy-Efficient Economy* , Washington, DC, USA, Tech. Rep. IEA-4EDNA, Apr. 2017.

[3] C. Goursaud and J. M. Gorce, "Dedicated networks for IoT : PHY / MAC state of theart and challenges", *EAI Trans. IoT* , vol. 1, no. 1, 2015.

[4] L. Vangelista, " Frequency Shift Chirp Modulation: The LoRa Modulation", *IEEE Signal Process. Lett.*, vol 24, no. 12, pp. 1818 - 1821, Dec. 2017.

[5] O. Georgiou and U. Raza, "Low Power Wide Area Network Analysis: Can LoRa Scale?", *IEEE Wireless Commun. Lett.*, vol. 6, no. 2, pp. 162 - 165, April 2017.

[6] A. Hoeller *et al.*. "Analysis and Performance Optimization of LoRa Networks With Time and Antenna Diversity", *IEEE Access*, vol. 6, pp. 32820 - 32829, 2018.

[7] D. Croce, M. Gucciardo, S. Mangione, G. Santaromita and I. Tinnirello, "Impact of LoRa Imperfect Orthogonality: Analysis of Link-Level Performance", *IEEE Commun. Lett.*, vol. 22, no. 4, pp. 796 - 799, April 2018.

[8] O. Afisiadis, M. Cotting, A. Burg and A. B.-Stimming, "On the Error Rate of the LoRa Modulation With Interference", *IEEE Trans. Wireless Commun.*, vol. 19, no. 2, pp. 1292 - 1304, Feb. 2020.

[9] Z. Qin, Y. Liu, G. Y. Li and J. A. McCann, "Performance Analysis of Clustered LoRa Networks", *IEEE Trans. Veh. Technol.*, vol. 68, no. 8, pp. 7616 - 7629, Aug. 2019.

[10] B. Su, Z. Qin and Qiang Ni, " Energy Efficient Resource Allocation for Uplink LoRa Networks ", *Proc. IEEE Global Communications Conference (GLOBECOM 2018)*, Abu Dhabi, United Arab Emirates, Dec. 2018.

[11] S. Dawaliby, A. Bradai and Y. Pousset, " Distributed Network Slicing in Large Scale IoT based on Coalitional Multi-Game Theory", *IEEE Trans. Netw. Service Manag.*, Early Access.

[12] M. Di Renzo, A. Zappone, L. T. Tu and M. Debbah, "System-Level Modeling and Optimization of the Energy Efficiency in Cellular Networks – A Stochastic Geometry Framework", *IEEE Trans. Wireless Commun.*, vol. 17, no. 4, pp. 2539 - 2556, Apr. 2018.

[13] M. Di Renzo, L. T. Tu, A. Zappone and M. Debbah, "A Tractable Closed-Form Expression of the Coverage Probability in Poisson Cellular Networks", *IEEE Wireless Commun. Lett.*, vol. 8, no. 1, pp. 249 - 252, Feb. 2017.

[14] Wolfram Mathematica document. [Online]. Available: http://functions.wolfram.com/06.06.21.0002.01.

[15] IEEE 802.16p-11/0014, *IEEE 802.16p Machine to Machine (M2M) Evaluation Methodology Document (EMD)*. [Online]. Available: http://ieee802.org/16/m2m/index.html

[16] N. Sornin, M. Luis, T. Eirich, T. Kramp and O. Hersent, *LoRaWAN Specifications*, LoRa Alliance, 2015.